Molecular Brain

RESEARCH

Open Access

Chronic corticosterone exposure causes anxiety- and depression-related behaviors with altered gut microbial and brain metabolomic profiles in adult male C57BL/6J mice

Hirotaka Shoji[1], Yasuhiro Maeda[2] and Tsuyoshi Miyakawa[1*]

Abstract

Chronic exposure to glucocorticoids in response to long-term stress is thought to be a risk factor for major depression. Depression is associated with disturbances in the gut microbiota composition and peripheral and central energy metabolism. However, the relationship between chronic glucocorticoid exposure, the gut microbiota, and brain metabolism remains largely unknown. In this study, we first investigated the effects of chronic corticosterone exposure on various domains of behavior in adult male C57BL/6J mice treated with the glucocorticoid corticosterone to evaluate them as an animal model of depression. We then examined the gut microbial composition and brain and plasma metabolome in corticosterone-treated mice. Chronic corticosterone treatment resulted in reduced locomotor activity, increased anxiety-like and depression-related behaviors, decreased rotarod latency, reduced acoustic startle response, decreased social behavior, working memory deficits, impaired contextual fear memory, and enhanced cued fear memory. Chronic corticosterone treatment also altered the composition of gut microbiota, which has been reported to be associated with depression, such as increased abundance of *Bifidobacterium*, *Turicibacter*, and *Corynebacterium* and decreased abundance of *Barnesiella*. Metabolomic data revealed that long-term exposure to corticosterone led to a decrease in brain neurotransmitter metabolites, such as serotonin, 5-hydroxyindoleacetic acid, acetylcholine, and gamma-aminobutyric acid, as well as changes in betaine and methionine metabolism, as indicated by decreased levels of adenosine, dimethylglycine, choline, and methionine in the brain. These results indicate that mice treated with corticosterone have good face and construct validity as an animal model for studying anxiety and depression with altered gut microbial composition and brain metabolism, offering new insights into the neurobiological basis of depression arising from gut-brain axis dysfunction caused by prolonged exposure to excessive glucocorticoids.

Keywords Corticosterone, Anxiety, Depression, Behavior, Gut microbiome, Metabolome, Mice

*Correspondence:
Tsuyoshi Miyakawa
miyakawa@fujita-hu.ac.jp
[1] Division of Systems Medical Science, Center for Medical Science, Fujita Health University, Toyoake, Aichi 470-1192, Japan
[2] Open Facility Center, Fujita Health University, Toyoake, Aichi 470-1192, Japan

Introduction

Exposure to stress activates the hypothalamic–pituitary–adrenal (HPA) axis, triggering the secretion of steroid hormones or glucocorticoids (cortisol in humans and corticosterone in mice) from the adrenal cortex. Glucocorticoids bind to glucocorticoid

receptors in the brain and are involved in physiological metabolism, immune responses, mood, and cognitive function [1–3]. Severe or prolonged stress can lead to HPA axis dysfunction and increased glucocorticoid levels, which have been implicated as significant risk factors in the pathogenesis of depression [4]. In mice, the administration of corticosterone (CORT) for a few weeks or more induces behavioral disturbances, which are reminiscent of the symptoms that characterize depression, such as increased anxiety-like and depression-related behaviors [5–17]. These findings suggest that mice chronically exposed to CORT are a valid animal model for studying depression.

The gut microbiota exerts a significant influence on various physiological processes in the host, such as the immune response, tryptophan metabolism, and neurotransmitter production [18–21], and is linked to behavior, affecting HPA responses and CORT levels [22–26]. Several lines of evidence have suggested that gut microbiome diversity is associated with neuropsychiatric and neurodegenerative disorders, including anxiety and depression [27]. Animal studies have shown that exposure to stress affects gut microbial composition [28, 29], and that chronic CORT treatment induces gut microbial changes, such as an increase in the abundance of the phylum Firmicutes and a decrease in the abundance of the phylum Bacteroidetes in cecal contents [30, 31]. Such CORT-induced changes in gut microbial composition may be a risk factor for behavioral disturbances and brain dysfunction, thus being considered a biomarker and a potential therapeutic target for depression. In animal facilities, various environmental factors can influence microbial composition [32]. Inter-facility variation could differentiate microbiome-disease associations, indicating the need for replicating findings from microbiome studies at multiple facilities [33].

Metabolomic profiling is a powerful tool for quantitatively measuring metabolic responses to normal or pathophysiological conditions and for uncovering significant biochemical signatures in diseases. A recent systematic review suggested that metabolomic changes in the blood and brain are implicated in the pathophysiology of depression [34]. Alterations in lipid metabolism in the liver were observed in mice chronically exposed to CORT, as indicated by elevated levels of oleic acid and palmitic acid [30]. Furthermore, a previous study demonstrated that rats administered chronic CORT showed changes in energy, lipid, and amino acid metabolism in whole brain samples [35]. The prefrontal cortex (PFC), hippocampus, habenula (Hb), paraventricular nucleus of the thalamus (PVT), and hypothalamus (Hypo), are among the brain regions associated with depression [36–39], However, what metabolomic changes in the specific brain regions are caused by chronic CORT exposure remain unknown.

In the present study, to evaluate mice chronically treated with CORT as an animal model of depression and to advance the understanding of the impact of chronic CORT exposure on brain function and mechanisms underlying depression, we investigated behavioral, gut microbial, and blood and brain metabolomic profiles of CORT-treated mice. There is a paucity of research on the effects of long-term exposure to CORT on some domains of behavior in mice, such as social behavior and learning and memory. Thus, we first investigated broad domains of behavior in adult male C57BL/6J mice chronically treated with CORT or vehicle (Veh) via drinking water for more than 4 weeks through 15 different behavioral tests to assess sensory and motor functions, locomotor activity in novel and familiar environments, anxiety-like and depression-related behaviors, social behaviors in novel and familiar environments, prepulse inhibition, working memory, spatial memory, and contextual and cued fear memory. Next, we measured plasma CORT levels to confirm the elevation of CORT after chronic oral administration of exogenous CORT. Additionally, we measured the weights of the adrenal glands, which play a critical role in CORT synthesis and secretion, as well as the thymus and spleen, which are involved in immune function, to assess the response of peripheral organs to repeated exogenous CORT administration. To examine the effects of CORT on the gut microbial composition, fecal samples were assessed using 16S rRNA gene amplicon sequencing. Finally, we investigated the plasma and brain metabolomic profiles of CORT- and Veh-treated mice. In addition to the HPA axis dysfunction hypothesis, there are various pathophysiological hypotheses for depression, such as monoamine deficiency, excitatory/inhibitory imbalance, and mitochondrial dysfunction hypotheses [40–43]. Therefore, in the metabolomic analysis, we sought to explore the concentrations of monoamines, glutamate and gamma-aminobutyric acid (GABA), amino acids, and some other metabolites in the brain regions associated with depression, including the PFC, Hb/PVT, hippocampus, hypothalamus, and plasma of chronic CORT- and Veh-treated mice.

Materials and methods

Animals

Male C57BL/6J mice 7 weeks old were purchased from the Jackson Laboratory Japan, Inc. (Kanagawa, Japan). After arrival at our animal facility, the mice were group-housed (four per cage) in plastic cages (250×182×139 mm; CLEA Japan, Inc., Tokyo, Japan) with paper chips for bedding (Paper Clean; Japan SLC, Inc., Shizuoka, Japan) covered with stainless-steel wire

lids and filter caps (CLEA Japan, Inc., Tokyo, Japan). Rooms were maintained under a 12-h light/dark cycle (lights on at 7:00 h) at 23 ± 2 °C. All animals were provided with food (CRF-1; Oriental Yeast Co., Ltd., Tokyo, Japan) and water *ad libitum* throughout the experiments. More than 2 weeks after arrival, oral administration of corticosterone solution or vehicle was initiated. All experimental procedures were approved by the Institutional Animal Care and Use Committee of Fujita Health University.

Corticosterone treatment

Corticosterone (95%, FUJIFILM Wako Pure Chemical Co., Japan) was dissolved in ethanol (99.5%, FUJIFILM Wako Pure Chemical Co., Japan) at 10 mg/mL and then mixed with filtered drinking water to a final concentration of 0.1 mg/mL CORT in 1% ethanol. Mice were divided into two groups: corticosterone (CORT)- and vehicle (Veh)-treated. The CORT-treated group had ad libitum access to a bottle of CORT solution. The Veh-treated group was given a water bottle containing a vehicle solution (1% ethanol in filtered drinking water). The solution in the bottle was changed every 3–7 days. Oral administration was continued until the end of the study, except for the sucrose preference test, as described below.

Behavioral tests

Four weeks after the beginning of CORT administration, CORT-treated mice (n = 20) and Veh-treated mice (n = 20) were subjected to a battery of behavioral tests in the following order (see Additional file 1: Table S1 for the test order and age of animals): general health and neurological screen, light/dark transition, open field, elevated plus maze, hot plate, social interaction, rotarod, startle response/prepulse inhibition, Porsolt forced swim, three-chamber social approach, T-maze spontaneous alternation, tail suspension, contextual and cued fear conditioning, sucrose preference, and home cage social interaction tests, as previously described [44, 45]. In addition, another group of mice received CORT or Veh solution for more than 4 weeks and were used for the Barnes maze test to assess spatial memory (CORT, n = 5; Veh, n = 10). After each test, the floors and walls of the test apparatus were cleaned with a 70% ethanol solution and hypochlorous acid water to prevent bias based on olfactory cues. Except for the sucrose preference test, behavioral tests were performed between 9:00 and 17:00.

General health and neurological screen

Physical characteristics, body weight, and rectal temperature were recorded. Neuromuscular strength was assessed by the grip strength and wire hang tests. Forelimb grip strength was measured using a grip strength meter (O'Hara & Co., Tokyo, Japan). The mice were lifted by their tails to grasp a wire grid with their forelimbs. They were then gently pulled back until they released the grid. The peak force of grip strength was recorded in Newtons (N). In the wire hang test, the mice were placed on a wire mesh (O'Hara & Co., Tokyo, Japan), which was inverted gently so that the subject grasped the wire. The latency to fall from the wire was recorded with a 60 s cut-off time.

Light/dark transition test

The light/dark transition test, developed by Crawley and colleagues [46] to assess anxiety-like behavior, was performed as previously described [47]. The apparatus consisted of a cage (21 × 42 × 25 cm) divided into two equal chambers by a partition with a door (O'Hara & Co., Tokyo, Japan). One chamber had white plastic walls and was brightly lit (390 lx) by lights mounted above the ceiling of the chamber. The other chamber had black plastic walls and was dark (2 lx). Both chambers had a white plastic floor. Mice were placed in the dark chamber and allowed to move freely between the two chambers for 10 min with the door open. Behavior was recorded using video cameras mounted on the ceiling. The distance traveled (cm), time spent in the light chamber (s), number of transitions, and latency to first enter the light chamber (s) were automatically calculated using the ImageLD program (see "Image analysis for behavioral test").

Open field test

The open field test was conducted in the open field apparatus with the VersaMax activity monitoring system (Accuscan Instruments, Columbus, OH, USA) to assess locomotor activity. The open field arena was made of acrylic with transparent walls and a white floor (40 × 40 × 30 cm). The floor of the center area, defined as 20 × 20 cm, was illuminated at 100 lx. Each mouse was placed in a corner of an open field and allowed to explore freely for 120 min. The distance traveled (cm), vertical activity (rearing measured by counting the number of photobeam interruptions), time spent in the center area (s), and stereotypic counts (beam-break counts for stereotyped behaviors) were calculated for each 5-min block.

Elevated plus maze test

The elevated plus maze test to assess anxiety-like behavior [48] was conducted as previously described [49, 50]. The apparatus consisted of two open arms (25 × 5 cm) and two closed arms of the same size with 15-cm-high transparent walls and a central square (5 × 5 cm) connecting the arms (O'Hara & Co., Tokyo, Japan). The floor of the apparatus was made of white plastic plates and was elevated to 55 cm above the floor. The open arms were

surrounded by a raised ledge (3-mm thick and 3-mm high) to prevent the mice from falling off the arms. Arms of the same type were placed opposite to one another. The illumination level in the central area was 100 lx. Each mouse was placed in the central square of the maze facing one of the closed arms. Distance traveled (cm), number of arm entries, percentage of entries into open arms, and percentage of time spent in open arms were measured using a video camera mounted above the apparatus during a 10-min test period. Data acquisition and analysis were performed automatically using the ImageEP program.

Hot plate test

The hot plate test was used to assess pain sensitivity to a thermal stimulus. Each mouse was placed on a hot plate (55.0 ± 0.1 °C; Columbus Instruments, Columbus, OH, USA) and the latency to a paw response (s) was recorded with a cut-off time of 15 s. The paw response was defined as either a paw lick or a foot shake.

Social interaction test

The social interaction test was performed to assess social behavior in a novel environment. Weight-matched mice (mean ± SD for differences in body weight between the two mice: CORT, 0.44 ± 0.22 g; Veh, 0.48 ± 0.23 g) from the same treatment group that had been housed in different cages were placed together in a white plastic box (40 × 40 × 30 cm; 100 lx at the center of the floor) together and allowed to explore it freely for 10 min. The total number of contacts, total duration of contacts (s), total duration of active contacts (measured when two mice made contact and one or both mice moved with a velocity of at least 10 cm/s), mean duration per contact (s), and total distance traveled (cm) were measured automatically using a video camera mounted above the apparatus and the image analysis program ImageSI.

Rotarod test

Motor coordination and balance were assessed in the rotarod test. The mice were placed on a rotating drum (3 cm diameter, Accelerating Rotarod; Ugo Basile, Varese, Italy). They were subjected to three trials per day for 2 consecutive days. The latency to fall from the rod (s) was measured. The rotarod speed was accelerated from 4 to 40 rpm over 300 s.

Three-chamber social approach test

The apparatus consisted of a rectangular, three-chambered box and a lid with a video camera (O'Hara & Co., Tokyo, Japan). Each chamber was made of white plastic (20 × 40 × 47 cm) and the partitions were made of transparent acrylic with a small square opening (5 × 3 cm). The three-chamber test was conducted as previously described [51]. In the first session, each test mouse was placed in the central chamber of the apparatus, which contained empty wire cages (9 cm in diameter and 11 cm in height, with vertical bars 0.5 cm apart) in the corners of each side chamber, and allowed to explore for 10 min (habituation session). Next, an unfamiliar C57BL/6J male mouse (stranger 1; 8–9 weeks old) that had no prior contact with the test mice was placed in the wire cage located in one of the side chambers. The location of the stranger mouse in the left and right chambers was systematically alternated between trials. First, the test mouse was placed in the central chamber and allowed to explore for a 10-min session to assess sociability (sociability test). Next, a second stranger mouse (stranger 2; 8–9 weeks old) was placed in the wire cage that had been empty during the first 10-min session to assess social preference for the new stranger (social novelty preference test). The test mouse had a choice between the first, already-investigated, now-familiar mouse (stranger 1) and the new, unfamiliar mouse (stranger 2). Time spent in each chamber and around each cage was automatically calculated from video images using the ImageCSI program.

Acoustic startle response/prepulse inhibition test

Startle response and prepulse inhibition tests were conducted using a startle reflex measurement system (O'Hara & Co., Tokyo, Japan), as previously described [52]. Briefly, the mice were placed in a clear plastic cylinder and left undisturbed in a sound-attenuating chamber for 10 min. A loud sound stimulus (110 or 120 dB, white noise, 40 ms) was then presented as a startle stimulus. A prepulse sound stimulus (74 or 78 dB, white noise, 20 ms) was presented 100 ms before the startle stimulus to assess prepulse inhibition. A test session consisted of six trial types (i.e., two types of startle stimulus-only trials, and four types of prepulse inhibition trials: 74–110, 78–110, 74–120, and 78–120 dB). Six blocks of the six trial types were presented in a pseudorandom order, such that each trial type was presented once within a block for 10 min. The average interval was 15 s (range: 10–20 s). A 70-dB white noise was presented as background noise during the test. The peak amplitude of the startle response to the stimuli was recorded for 400 ms from the onset of the prepulse stimulus. The percentage PPI was calculated for each mouse using the following formula: percent PPI = 100 × [1 − (startle response amplitude in prepulse + startle trial)/(startle response amplitude in startle stimulus-only trial)].

Porsolt forced swim test

The Porsolt forced swim test [53] was used to assess depression-related behavior. Mice were placed in a clear

plastic cylinder (20 cm height × 10 cm diameter, O'Hara & Co., Tokyo, Japan) filled with water (approximately 21 °C) to a depth of 8 cm for a 10 min per day for 2 consecutive days. The percentage of immobility time was automatically recorded using the ImagePS/TS program as previously described [54, 55].

T-maze spontaneous alternation test

The T-maze spontaneous alternation test was conducted to assess spatial working memory using a modified automatic T-maze apparatus (O'Hara & Co.), as previously described [44, 56]. The apparatus consisted of white plastic runways with 25-cm-high walls. It was partitioned into six areas: the stem of the T, a straight runway, the left and right arms, and the connecting passageways from the arms to the stem of the T. Mice were subjected to a session consisting of 10 trials per day for 3 days (a cut-off time of 50 min). Each trial consisted of a forced-choice run followed by a free-choice run (inter-trial interval, 60 s). In the forced-choice run, mice were forced to enter either the left or the right arm of the T-maze and were held in that arm for 10 s. After the 10 s, the doors of the passageway connecting the arm to the stem of the T were opened, and the mouse could return to the start compartment. A free-choice run began 3 s after the mice entered the start compartment. The mice were allowed to choose one of the arms in the free-choice run, and if the mice entered the arm opposite to the arm that the mice entered in the forced-choice run, the response was recorded as a correct response. Data acquisition and analysis were performed automatically using the ImageTM program (see "Image analysis for behavioral test").

Tail suspension test

The tail suspension test was performed to assess depression-related behavior [57]. Mice were suspended 30 cm above the floor in a visually isolated area, using adhesive tape placed approximately 1 cm from the tip of the tail. Immobility time was recorded for 10 min using the ImagePS/TS program in the same manner as for the forced swim test.

Contextual and cued fear conditioning test

The contextual and cued fear conditioning test was conducted to assess fear memory using an automated video analysis system, as previously described [58]. First, mice were placed in a conditioning chamber (26 × 34 × 29 cm) and allowed to explore freely for 2 min. The animals were then presented with an auditory cue (55-dB white noise), which served as a conditioned stimulus (CS) for 30 s. During the last 2 s of the CS, the mice received a mild footshock (0.3 mA, 2 s) as an unconditioned stimulus (US). Two more CS–US pairings were presented at 120-s intervals. One day and 28 days after the conditioning session, a context test was performed in the conditioning chamber, in which the mice were allowed to explore for 5 min. A cued test in an altered context was then performed in a triangular box (35 × 35 × 40 cm) made of opaque white plastic located in another sound-attenuated room more than 3 h after the context test. In the cued test, after an initial 3-min period without CS presentation, the CS was presented during the last 3-min period. For each test, video images were recorded at one frame per second. Freezing time (%) and distance traveled (cm) were automatically measured in each trial using the ImageFZ program. Images were also recorded at a rate of 4 frames per second for 6 s from 2 s before the application of a 2-s footshock to 2 s after the footshock, and distance traveled (cm) was measured as an index of footshock sensitivity.

Sucrose preference test

Mice were individually housed in plastic cages (250 × 182 × 139 mm) with fresh paper chips for bedding and were given two bottles of filtered tap water 7 days after the first contextual and cued fear conditioning test. The following day, the mice were given one bottle of water and a second bottle of 1% sucrose solution. The bottles were weighed at approximately 24-h intervals to measure water and sucrose intake over 4 days, with the left–right position changed daily. Sucrose preference was expressed as 100 × [(sucrose intake averaged over 4 days)/(sucrose intake averaged over 4 days + water intake averaged over 4 days)]. The mice were not given CORT or vehicle solutions in the test.

Home cage social interaction test

The home cage social interaction test was conducted to assess social behavior and activity levels under familiar conditions in a home cage for 7 days. The social interaction monitoring system consisted of a home cage with paper chips as bedding and a cage top with an infrared video camera (25 × 15 × 23.5 cm, interior dimensions). Weight-matched mice of the same treatment group housed in separate cages, were housed together in the cage (mean ± SD for the differences in the body weight between the two mice: CORT, 0.50 ± 0.25 g; Veh, 0.42 ± 0.41 g). Video images at a rate of 1 frame per second were analyzed to assess social interaction by automatically counting the number of particles (animals) detected in each frame using the ImageHA program (one particle indicates contact between two mice, and two particles indicate that mice are not in contact with each other). Activity was quantified by measuring the number of pixels that changed between each pair of consecutive

images. The mean number of animals and total activity level in each 1-h bin were calculated for 1 week.

Barnes maze test

The Barnes circular maze test [59] was conducted to test spatial reference memory on "dry land," a white circular surface, 1.0 m in diameter, with 12 holes equally spaced around the perimeter (O'Hara & Co., Tokyo, Japan). The circular open field was elevated 75 cm above the floor. A black Plexiglas escape box (17 × 13 × 7 cm) was located under one of the holes (target hole). In the acquisition session, two trials per day were conducted for 9 days. Each mouse was placed in the center of the maze in each trial and then allowed to explore it. If the mouse did not enter the escape box for a maximum of 5 min, it was gently guided to the escape hole. After entering the escape hole, the mouse remained in the escape box for 30 s before returning to the holding cage. The target's location was consistent for a given mouse but randomized across mice. The maze was rotated daily, with the target's spatial location unchanged for distal visual cues, to prevent bias based on olfactory or proximal cues. The latency to first reaching the target hole (s), number of errors to reach the target hole, distance traveled first to reach the target hole (cm), and number of omissions (visit to the target hole without subsequent entry into the target hole) were recorded automatically by the ImageBM program. One day and 28 days after the last acquisition session, probe trials were performed without the escape box to assess spatial reference memory. In the probe test, the time spent around each hole (s) was measured using the ImageBM program.

Image analysis for behavioral test

Image analysis programs (ImageLD/EP/SI/CSI/PS/TS/TM/BM/FZ/HA) were used to analyze mouse behaviors automatically, as previously described [47, 49, 56, 58]. The programs, based on the public domain ImageJ software (developed by Wayne Rasband at the National Institute of Mental Health, Bethesda, US), were modified by Tsuyoshi Miyakawa. The ImageLD/EP/TM/FZ programs can be freely downloaded from the "Mouse Phenotype Database" (http://www.mouse-phenotype.org/).

Assessment of food and solution intake

Food intake was measured weekly by weighing the food pellets in each cage (CORT, n = 5 cages; Veh, n = 5 cages) for 8 weeks from the beginning of the CORT and Veh treatments. Mean food intake (g) per mouse per day was calculated. Water bottles were also weighed in each cage, and mean solution intake (g) per mouse per day was calculated.

Measurement of adrenal gland, thymus, and spleen weights

Adrenal glands, thymus, and spleen were collected from an independent cohort of mice after 6 weeks of treatment with CORT or vehicle (CORT, n = 10; Veh, n = 12). Organs were weighed immediately after collection. Relative weight of each organ was calculated by dividing the organ weight (mg) by body weight (g).

Plasma corticosterone measurement

Mice treated with CORT or vehicle for 4 weeks (CORT, n = 12; Veh, n = 16) were used to assess stress response by measuring plasma CORT levels after the tail suspension test. Seven CORT-treated mice and eight Veh-treated mice were subjected to the tail suspension test for 10 min. Immediately after the test, A total of 200 µL of blood was collected from the facial or submandibular veins within 30 s of holding the mouse using a Goldenrod Animal Lancet (MEDIpoint, Inc., NY, USA). Similarly, blood was collected from the remaining mice that were experimentally naïve immediately after they were taken from their home cages. In our previous study, basal CORT levels measured from blood samples using the Animal Lancet [50, 60] were similar to those measured from trunk blood collected immediately after cervical dislocation and decapitation under stress-free conditions [61]. Thus, it is unlikely that the use of Animal Lancet influences CORT levels. Blood samples were placed into tubes containing 10 µL of heparin/saline solution (100 Units/mL) and temporarily stored on ice. They were then centrifuged at 3000×*g* for 10 min at 4 °C. Supernatants were collected and stored at − 80 °C until measurement. Plasma CORT concentrations were determined according to the manufacturer's protocol, using an enzyme immunoassay kit (Assay Designs Inc., MI, USA).

Fecal microbiome analysis

Fecal samples were collected from the colon of an independent group of mice (CORT, n = 8; Veh, n = 8) after cervical dislocation after 5 weeks of treatment. The samples were placed in tubes and stored at − 80 °C. DNA from fecal samples was extracted by a bead-based method, as previously described [62]. Prokaryote universal primers (Pro341F and Pro805R) with the sample-specific 8-bp dual-index barcode sequences were used to amplify V3 and V4 regions of 16S rDNA genes by polymerase chain reaction [62, 63]. The barcoded amplicons were paired-end sequenced on the Illumina MiSeq platform using the MiSeq Reagent Kit v3 (600 cycles, 2 × 284-bp cycle; Illumina, San Diego, CA, USA). Paired-end reads were joined using the fastq-join program [64]. The joined reads with a quality value score ≥ 20 for > 99% of the

sequence were extracted using FASTX-Toolkit [65] and were used for further analysis. The chimeric sequences were removed using uSearch61 software [66, 67]. Taxonomy assignment from the sequence reads was performed using Metagenome@KIN software (World Fusion, Tokyo, Japan) and the database RDP MultiClassifier ver.2.11 [68] with an 80% confidence level. The amplicon sequencing and taxonomic assignment were performed by Techno-Suruga Laboratory Co., Ltd. (Shizuoka, Japan).

The read counts were analyzed for assessing α-diversity (species richness and evenness from the rarefied counts; observed number of microbial genera, Chao1 index, and Shannon indexe) using R packages 'vegan' (ver. 2.5-7) [69]. In addition, β-diversity was visualized with principal coordinate analysis (PCoA) with Bray–Curtis dissimilarity and the percentage of variance explained by the PCoA axis was calculated using the pcoa function in the R software package 'ape.' Permutational multivariate analysis of variance (PERMANOVA) was used to assess the differences using the adonis function in the R package 'vegan.' Furthermore, the relative abundance of the microbiota at the genus level was analyzed using the linear discriminant analysis (LDA) effect size (LEfSe) method [70] to identify taxonomic features characterizing the differences between the two treatment groups (LDA score > 3, $p < 0.05$).

Plasma and brain metabolomic analysis

Eight CORT-treated and seven Veh-treated mice were euthanized by cervical dislocation on the 40th day of treatment. Immediately after decapitation, approximately 300 µL of trunk blood was collected in a tube containing heparin solution and temporarily stored on ice until plasma collection. Brains were removed and placed on an ice-cold glass plate to minimize possible metabolic changes. The medial prefrontal cortex (mPFC), habenula, and paraventricular nucleus of the thalamus (Hb/PVT), dentate gyrus (DG) and CA of the hippocampus, and hypothalamus (Hypo) were quickly dissected, collected in tubes, frozen in liquid nitrogen, and then stored at − 80 °C in a freezer until use (for the weight of brain tissue, see Table S2). The procedure from picking up the mouse to freezing the brain samples took approximately 10 min for each mouse.

Concentrations of metabolites were determined by high-performance liquid chromatography–tandem mass spectrometry (HPLC–MS/MS). All steps of tissue sample extraction were performed on ice. To brain samples was added 10 µmol/L 2-morpholinoethanesulfonic acid (internal standard) in methanol (500 µL for 50 mg of tissue). The samples were homogenized using an ultrasonic homogenizer (THU-80; AS ONE Co., Osaka, Japan), and water (250 µL for 50 mg of tissue) and chloroform (400 µL for 50 mg of tissue) were then added. After the mixture was centrifuged at 4 °C and 15,000×*g* for 15 min, the supernatant was filtered using a 10 kDa cutoff filter (Amicon Ultra centrifugal filter; Merck Millipore, Bulington, MA, USA). The filtrate was lyophilized and the precipitate was dissolved in 50 µL of water, after which it was subjected to HPLC–MS/MS (LCMS-8060; Shimadzu Co., Kyoto, Japan). Metabolites were eluted from a reverse phase column (Discovery HS F5, 150 × 2.1 mm, 3 µm; Supelco, Bellefonte, PA, USA) with the gradient method using a mobile phase with 0.1% formic acid in water and 0.1% formic acid in acetonitrile at a flow rate of 0.25 mL/min, and were then analyzed in electronspray ionization (ESI) positive or negative ion multiple reaction monitoring (MRM) mode of MS/MS. The Q1 or Q3 pre bias voltages, collision energies and mass transitions used are listed in Table S3. The MS–MS data of metabolites were analyzed using principal component analysis (PCA) and partial least square-discriminant analysis (PLS-DA) to visualize group differences in the metabolites. Metabolites that contribute to group classification were selected using the criteria of a variable importance in projection (VIP) score of the PLS-DA greater than 1.0, and an unadjusted p-value of less than 0.05, which have been used as a widely accepted standard in metabolomic studies. The selected metabolites were used for enrichment (over-representation) analysis through MetaboAnalyst 5.0 [71].

Statistical analysis

Statistical analyses were performed using SAS Studio (SAS OnDemand for Academics; SAS Institute, Cary, NC, USA) and R (version 3.6.3). Behavioral data were analyzed using Student's t-test or two-way repeated-measures ANOVAs with treatment as a between-subject variable and trial/time/block as a within-subject variable. When a treatment × trial/time/block interaction was significant, simple main effect analyses were conducted to examine the treatment effect at each time point. Microbial and metabolite abundances were analyzed by the Mann–Whitney U test and Student's t-test using SAS and R packages described above. Comparisons of organ weights and plasma corticosterone levels between treatment groups were performed using Student's t-test or two-way ANOVA. Statistical significance level was set at 0.05. Values in graphs are expressed as mean ± SEM.

Results

Physical characteristics and neurological functions in CORT-treated mice

The battery of behavioral tests was performed after 4 to 14 weeks of CORT treatment (see Additional file 1: Table S1). The statistical results of behavioral data

from CORT- and Veh-treated mice are summarized in Table S4.

CORT-treated mice showed increased body weight (Fig. 1a: 4-week treatment, $t_{38}=4.44$, $p<0.0001$; Additional file 2: Fig. S1a: 12-week treatment, $t_{32}=3.65$, $p=0.0009$), increased food intake (Additional file 2: Fig. S1b; $F_{1,8}=35.77$, $p=0.0003$; interaction, $F_{7,56}=4.12$, $p=0.0010$), and solution intake (Additional file 2: Fig. S1c; $F_{1,8}=131.96$, $p<0.0001$; interaction, $F_{7,56}=10.56$, $p<0.0001$) compared to Veh-treated mice. CORT-treated mice showed increased rectal temperature after 4 weeks of treatment (Fig. 1b: $t_{38}=2.39$, $p=0.0218$). Reduced rotarod latency was observed in CORT-treated mice (Fig. 1f: treatment, $F_{1,38}=34.66$, $p<0.0001$; interaction, $F_{5,190}=1.36$, $p=0.2411$), suggesting that chronic CORT treatment caused motor dysfunction or decreased motivation to perform the task. There were no significant effects of treatment on grip strength (Fig. 1c: $t_{38}=1.44$, $p=0.1594$), wire hang latency (Fig. 1d: $t_{38}=0.62$, $p=0.5394$), or hot plate latency (Fig. 1e: $t_{38}=0.66$, $p=0.5160$), indicating no differences in muscular strength and thermal pain sensitivity between the treatment groups. The prepulse inhibition test showed that acoustic startle responses at 110 and 120 dB sound stimuli and prepulse inhibition of the startle response at 74–120 dB trials were lower in CORT-treated mice than in Veh-treated mice (Fig. 1g, h: 110 dB, $t_{36}=4.74$, $p<0.0001$; 120 dB, $t_{36}=3.89$, $p=0.0004$; 74–110 dB, $t_{36}=0.03$, $p=0.9770$; 78–110 dB, $t_{36}=1.35$, $p=0.1855$; 74–120 dB, $t_{36}=2.18$, $p=0.0361$; 78–120 dB, $t_{36}=1.46$, $p=0.1534$).

Increased anxiety-like and depression-related behaviors in CORT-treated mice

CORT-treated mice showed a lower number of transitions between the light and dark chambers than Veh-treated mice in the light/dark transition test (Fig. 2c: $t_{38}=2.03$, $p=0.0497$), while there were no statistically significant differences in the distance traveled in the dark and light chambers (Fig. 2a: dark, $t_{38}=2.01$, $p=0.0515$; light, $t_{38}=1.21$, $p=0.2354$), time spent in the light chamber (Fig. 2b: $t_{38}=0.21$, $p=0.8319$), and latency to enter

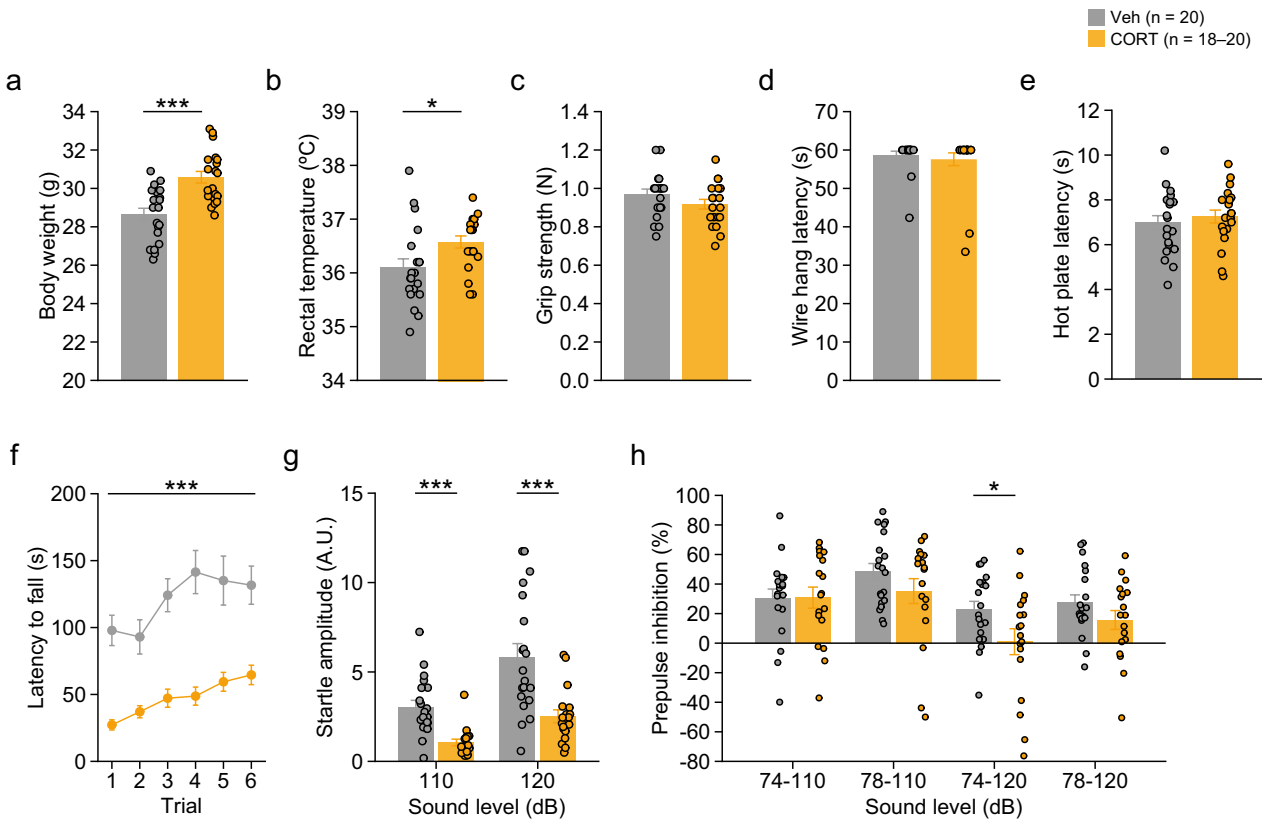

Fig. 1 Body weight, body temperature, muscular strength, sensitivity to thermal stimulus, motor function, and prepulse inhibition in mice chronically treated with corticosterone. **a** Body weight (g), **b** body temperature (°C), **c** grip strength (Newton, N), **d** latency to fall off the wire (s) in the wire hang test, **e** latency to response to thermal stimulus (s) in the hot plate test, **f** latency to fall off the rod in the rotarod test, **g** acoustic startle response to loud noise (110 and 120 dB white noise), and **h** prepulse inhibition of the startle response with a prepulse of either 74 or 78 dB white noise in CORT- and Veh-treated mice. Values are means ± SEM. *p < 0.05. ***p < 0.001

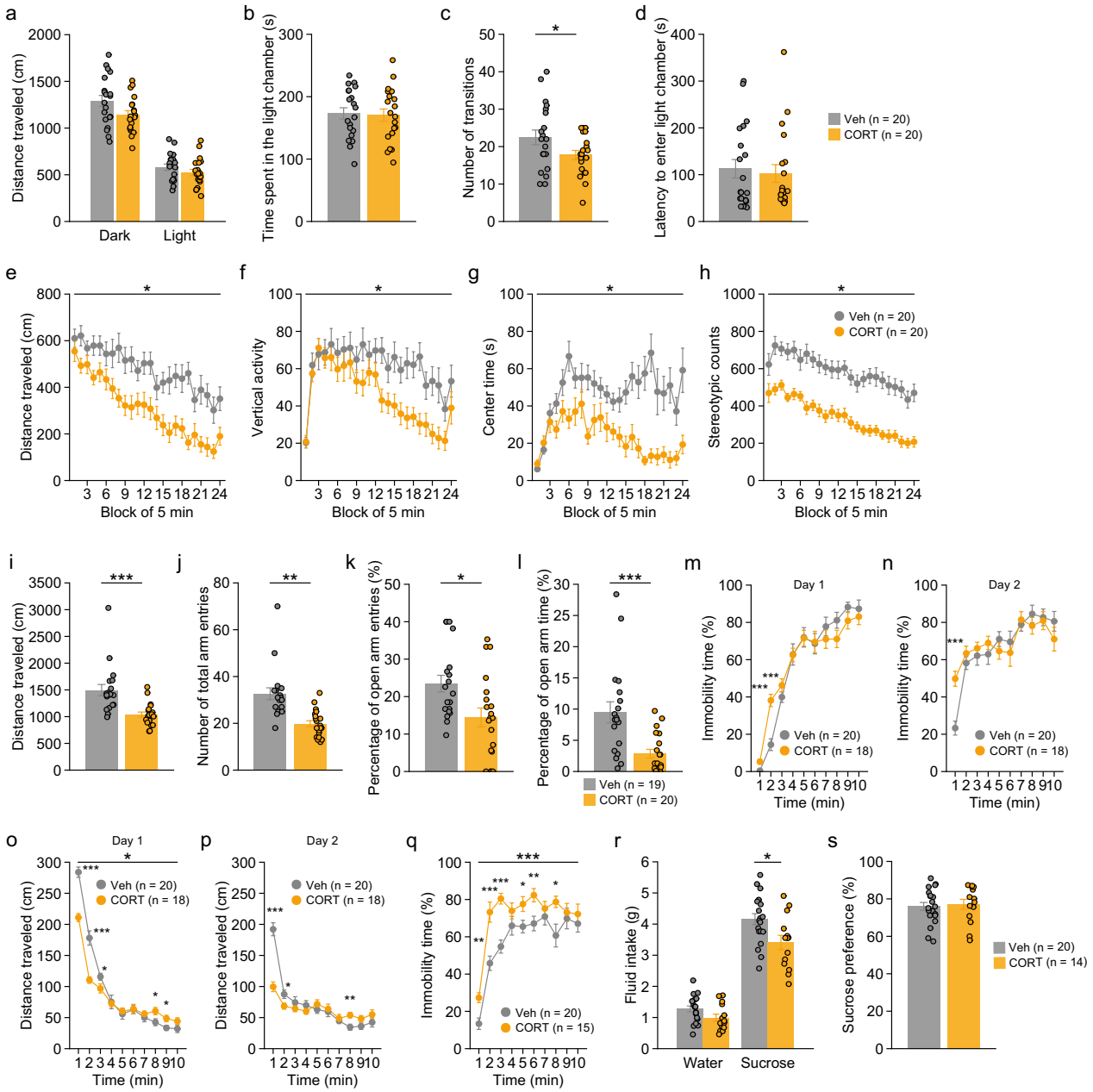

Fig. 2 Locomotor activity and anxiety-like and depression-related behaviors in mice chronically treated with corticosterone. **a**–**d** Light/dark transition test: **a** distance traveled (cm) in the dark and light chambers, **b** time spent in the light chamber (s), **c** number of transitions, and **d** latency to enter the light chamber (s). **e**–**h** Open field test: **e** distance traveled (cm), **f** vertical activity, **g** time spent in the center area (s), and **h** stereotypic counts. **i**–**l** Elevated plus maze test: **i** total distance traveled (cm), **j** number of total arm entries, **k** percentage of open arm entries (%), and **l** percentage of time spent in the open arms. **m**–**p** Porsolt forced swim test: **m**, **n** percentage of immobility time (%) and **o**, **p** distance traveled (cm) in ten 1-min blocks of the test session on test days 1 and 2. **q** Percentage of immobility time (%) in the tail suspension test. **r**, **s** Sucrose preference test: **r** water and sucrose solution intake (g) and **s** percentage of sucrose preference (%). Values are means ± SEM. *p < 0.05. **p < 0.01. ***p < 0.001

the light chamber (Fig. 2d: $t_{38} = 0.37$, $p = 0.7147$) between treatment groups. In the open field test, CORT-treated mice exhibited significant reductions in distance traveled (Fig. 2e: $F_{1,38} = 11.20$, $p = 0.0019$), vertical activity (Fig. 2f: $F_{1,38} = 5.19$, $p = 0.0284$), time spent in the center area (Fig. 2g: $F_{1,38} = 25.27$, $p < 0.0001$), and stereotypic counts (Fig. 2h: $F_{1,38} = 35.53$, $p < 0.0001$) compared to Veh-treated mice. In the elevated plus maze test, CORT-treated mice also showed decreases in distance traveled (Fig. 2i: $t_{37} = 4.05$, $p = 0.0003$), number of total arm

entries (Fig. 2j: $t_{37}=4.56$, $p<0.0001$), percentage of open arm entries (Fig. 2k: $t_{37}=2.67$, $p=0.0112$), and percentage of time on open arms (Fig. 2l: $t_{37}=3.70$, $p=0.0007$) compared to Veh-treated mice. These results suggest that chronic CORT treatment decreases locomotor activity and increases anxiety-like behavior.

In the forced swim test, there were significant treatment × time interactions for the percentage of immobility time (Fig. 2m: treatment, $F_{1,36}=0.05$, $p=0.8186$; interaction, $F_{9,324}=3.09$, $p=0.0014$) and distance traveled (Fig. 2o: treatment, $F_{1,36}=4.82$, $p=0.0346$; interaction, $F_{9,324}=13.06$, $p<0.0001$) on day 1. Similar results were found on day 2 for immobility (Fig. 2n: treatment, $F_{1,36}=0.39$, $p=0.5372$; interaction, $F_{9,324}=2.49$, $p=0.0093$) and distance traveled (Fig. 2p: treatment, $F_{1,36}=2.90$, $p=0.0973$; interaction, $F_{9,324}=12.27$, $p<0.0001$). Then, simple main effect analysis revealed that CORT-treated mice exhibited increased immobility compared to Veh-treated mice in the first and second time bin on day 1 (all $p<0.001$) and in the first time bin on day 2 ($p<0.0001$), and CORT-treated mice also showed a significantly shorter distance traveled than Veh-treated mice on days 1 and 2 (Fig. 2o, p: $p<0.05$). In addition, increased immobility in CORT-treated mice was observed in the tail suspension test (treatment, $F_{1,33}=24.08$, $p<0.0001$; interaction, $F_{9,297}=2.08$, $p=0.0309$) in several time bins during the 10-min test (Fig. 2q: $p<0.05$). In the sucrose preference test, CORT-treated mice consumed a decreased volume of sucrose solution compared to Veh-treated mice (Fig. 2r: $t_{32}=2.63$, $p=0.0132$), suggesting anhedonia-like behavior, although there were no statistically significant differences in water intake (Fig. 2r: $t_{32}=1.92$, $p=0.0644$) and the percentage of sucrose preference (Fig. 2s: $t_{32}=0.34$, $p=0.7361$) between treatment groups. Together, these data indicate increased depression-related behavior in CORT-treated mice.

Decreased social behavior in CORT-treated mice

In the social interaction test, two mice from different cages in the same treatment group were placed in a novel chamber. CORT-treated mice exhibited a trend toward a decreased number of contacts (Fig. 3a: $t_{18}=2.10$, $p=0.0504$), a shorter duration of active contacts (Fig. 3c: $t_{18}=2.70$, $p=0.0146$), and a shorter distance traveled (Fig. 3e: $t_{18}=4.32$, $p=0.0004$) compared to Veh-treated mice. These data indicate that chronic CORT treatment decreased the frequency of social interaction, although the contact duration per contact was increased (Fig. 3d: $t_{18}=2.58$, $p=0.0189$). There was no significant treatment effect on the total duration of contacts (Fig. 3b: $t_{18}=0.06$, $p=0.9542$).

In the three-chamber sociability test, Veh-treated mice spent a longer time in the chamber with the cage containing stranger 1 than in the chamber containing an empty cage (Fig. 3f: $t_{19}=6.87$, $p<0.0001$), and spent a longer time around the cage containing stranger 1 than around the empty cage (Fig. 3g: $t_{19}=7.23$, $p<0.0001$), whereas CORT-treated mice showed no significant differences between the time spent in the chambers (Fig. 3f: $t_{18}=1.58$, $p=0.1314$) and time around cages (Fig. 3g: $t_{18}=1.93$, $p=0.0692$) during the first 5-min period. These results indicate that CORT-treated mice displayed no preference for a novel mouse. During the last 5-min period of the sociability test, the preference for chamber or cage containing stranger 1 was observed in both Veh-treated mice (for time in chamber, $t_{19}=2.13$, $p=0.046$; for time around cage, $t_{19}=1.38$, $p=0.1814$) and CORT-treated mice (for time in chamber, $t_{18}=4.12$, $p=0.0006$; for time around cage, $t_{18}=3.83$, $p=0.0012$).

In the three-chamber social novelty preference test, Veh-treated mice spent a longer time in the chamber and around the cage with stranger 2 than with stranger 1 during the first 5-min period (Fig. 3h, i: for time in chamber, $t_{19}=3.34$, $p=0.0034$; for time around cage, $t_{19}=3.38$, $p=0.0031$). Similar results were found in CORT-treated mice during the first 5-min period (Fig. 3h and i: for time in chamber, $t_{18}=2.13$, $p=0.0464$; for time around cage, $t_{18}=1.94$, $p=0.0673$). During the last 5-min period, there were no significant differences between the time spent in the chamber with stranger 2 and the time spent in the chamber with stranger 1, or between the time spent around the cage containing stranger 2 and the time spent around the cage containing stranger 1, in both Veh-treated mice (for time in chamber, $t_{19}=0.45$, $p=0.6547$; for time around cage, $t_{19}=0.21$, $p=0.8294$) and CORT-treated mice (chamber, $t_{18}=0.86$, $p=0.3972$; for time around cage, $t_{18}=0.48$, $p=0.6365$).

Pairs of mice from different cages of the same treatment group that had not been encountered previously were housed together in a cage and left for 7 days to measure locomotor activity and social interaction in a home cage. In the home cage social interaction test, there were significant main effects of treatment and significant treatment × time interactions in the number of particles (one particle indicates contact between the two mice, and two particles indicate that the mice are not in contact with each other) (Fig. 3j: treatment, $F_{1,13}=7.56$, $p=0.0166$; interaction, $F_{167,2171}=1.94$, $p<0.0001$) and the activity level (Fig. 3l: treatment, $F_{1,13}=15.63$, $p=0.0017$; interaction, $F_{167,2171}=3.15$, $p<0.0001$). To assess social interaction following an acclimation in the cage, the number of particles and activity levels were averaged over the last 3 days. There were significant main effects of treatment and significant treatment × time interactions

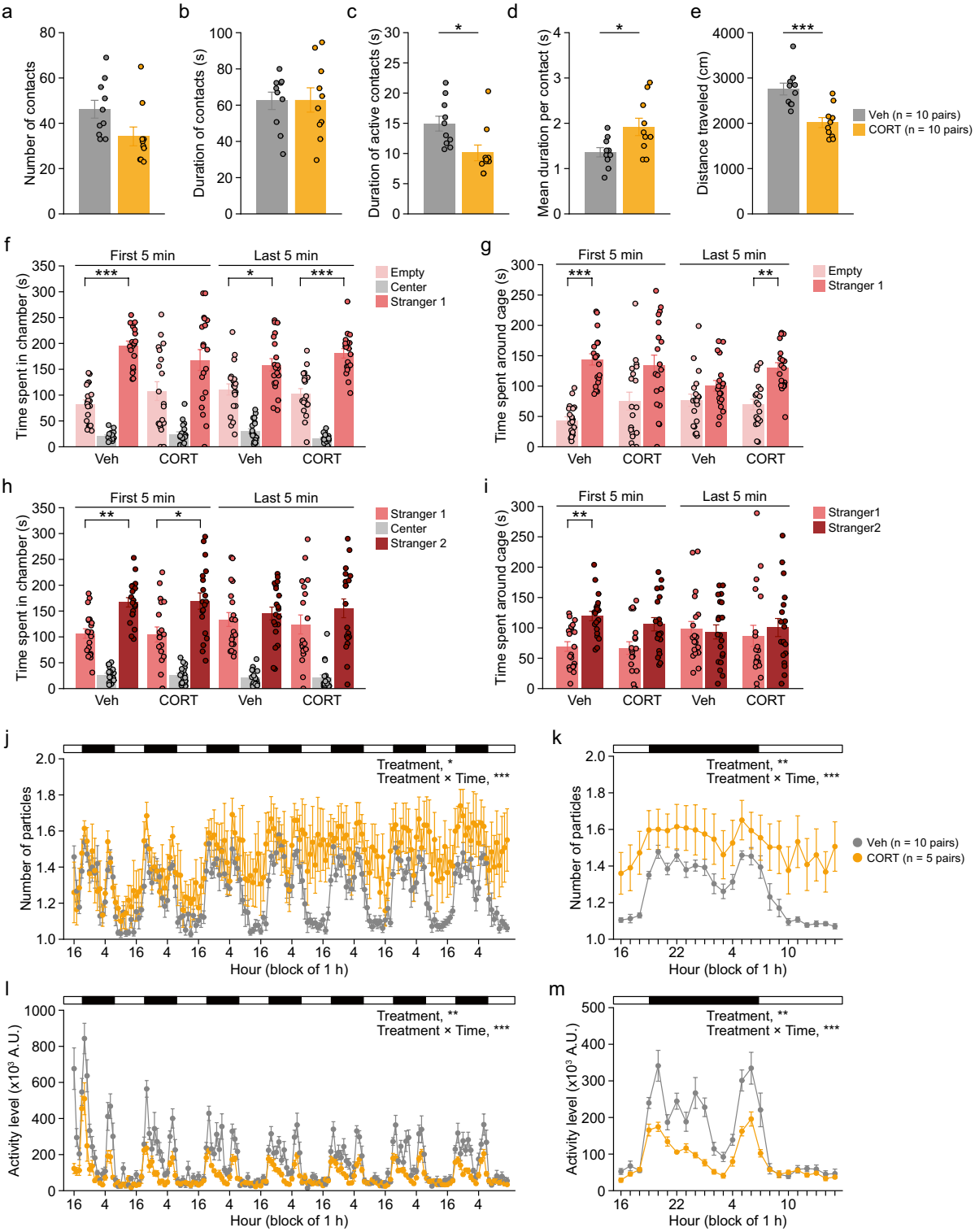

Fig. 3 Social behavior of mice chronically treated with corticosterone. **a**–**e** Social interaction test: **a** number of contacts, **b** duration of contacts (s), **c** duration of active contacts (s), **d** mean duration per contact (s), and **e** total distance traveled (cm). **f**, **g** Three-chamber sociability test: **f** time spent in chambers (s) and **g** time spent around the cage (s). **h**, **i** Three-chamber social novelty preference test: **h** time spent in the chamber (s) and **i** time spent around the cage (s). **j**–**m** Home cage social interaction test: **j** number of particles (two particles indicated that the mice were not in contact with each other, and one particle indicated contact between the two mice) in 1-h bin for 7 days, **k** number of particles averaged over the last 3 days, **l** activity level in 1-h bin for 7 days, and **m** activity level averaged over the last 3 days. Values are means ± SEM. *p < 0.05. **p < 0.01. ***p < 0.001

in the average number of particles (Fig. 3k: treatment, $F_{1,13}=9.17$, $p=0.0097$; interaction, $F_{23,299}=2.51$, $p=0.0002$) and the average activity level (Fig. 3m: treatment, $F_{1,13}=11.94$, $p=0.0043$; interaction, $F_{23,29}9=4.37$, $p<0.0001$). A significantly greater number of particles was found in CORT-treated mice than in Veh-treated mice in the time period of 16–19, 21, 23, 2–4, and 8–15 (Fig. 3k: $p<0.05$). Lower activity levels were observed in CORT-treated mice in the time period of 19, 20, 22–1, and 5–7 (Fig. 3m: $p<0.05$). These data indicate that CORT-treated mice exhibited reduced social contacts and decreased activity in the familiar environment.

Decreased spontaneous alternation behavior in CORT-treated mice

CORT-treated mice displayed reduced spontaneous alternation, as indicated by the lower percentage of correct responses compared to Veh-treated mice in the T-maze test (Fig. 4a: $F_{1,34}=4.26$, $p=0.0466$), which is suggestive of reduced working memory. CORT-treated mice took a longer time to complete a session than Veh-treated mice (Fig. 4b: $F_{1,34}=18.29$, $p=0.0001$). There was no significant difference in the distance traveled to complete the session between the treatment groups (Fig. 4c: $F_{1,34}=0.23$, $p=0.6370$).

Altered fear-related behavior in CORT-treated mice

During the conditioning session of the fear conditioning test, CORT-treated mice exhibited higher freezing (Fig. 4d: treatment, $F_{1,30}=13.64$, $p=0.0009$; interaction, $F_{7,210}=4.36$, $p=0.0002$) and shorter distance traveled (Additional file 3: Fig. S2a: treatment, $F_{1,30}=13.06$, $p=0.0011$; interaction, $F_{7,210}=1.82$, $p=0.0845$) than Veh-treated mice. The increased freezing was observed during the first minute and from the third to seventh minutes of the conditioning session before and after CS–US presentation, which indicates the possibility of suppressed exploration or increased anxiety in the novel environment and increased fear to footshock in CORT-treated mice. During the 2-s period of US presentation, CORT-treated mice traveled shorter distances than Veh-treated mice (Additional file 3: Fig. S2f–h: for US1, $F_{1,30}=5.42$, $p=0.0268$; for US2, $F_{1,30}=3.48$, $p=0.0719$; for US3, $F_{1,30}=8.70$, $p=0.0061$), suggesting decreased sensitivity to footshock in CORT-treated mice.

One day after the conditioning, CORT-treated mice showed significantly lower

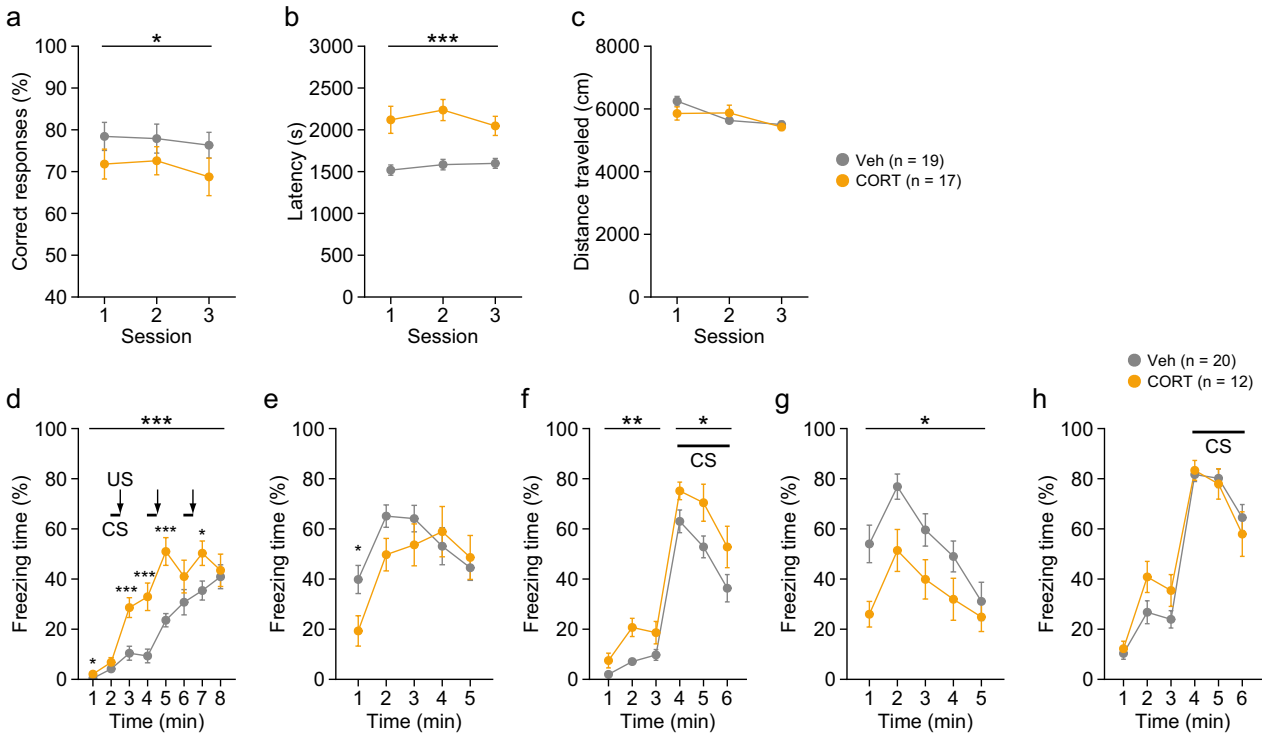

Fig. 4 Spontaneous alternation and fear conditioning in mice chronically treated with corticosterone. **a**–**c** T-maze spontaneous alternation test: **a** correct responses (%), **b** latency to complete a session (s), and **c** total distance traveled (cm) to complete a session. **d**–**h** Fear conditioning test: freezing time (%) in the conditioning session on day 1 (**d**), context test on day 2 (**e**), cued test on day 2 (**f**), context test on day 29 (**g**), and cued test on day 29 (**h**). Values are means ± SEM. *$p<0.05$. **$p<0.01$. ***$p<0.001$

freezing (Fig. 4e: treatment, $F_{1,30}=1.00$, $p=0.3251$; interaction, $F_{4,120}=2.83$, $p=0.0276$) and greater distance traveled (Additional file 3: Fig. S2b: treatment, $F_{1,30}=5.75$, $p=0.0229$; interaction, $F_{4,120}=5.07$, $p=0.0008$) than Veh-treated mice in the context test. Similar results were observed 28 days after the conditioning for freezing (Fig. 4g: treatment, $F_{1,30}=7.35$, $p=0.0110$; interaction, $F_{4,120}=1.07$, $p=0.3725$) and distance traveled (Additional file 3: Fig. S2d: treatment, $F_{1,30}=9.05$, $p=0.0053$; interaction, $F_{4,120}=1.39$, $p=0.2401$) in the same context. These data raise two possibilities: an increase in escape response to the context and a reduction in both recent and remote contextual fear memory in CORT-treated mice.

In the cued test conducted 1 day after the conditioning, increased freezing was observed in CORT-treated mice during the pre-CS period (Fig. 4f: treatment, $F_{1,30}=12.63$, $p=0.0013$; interaction, $F_{2,60}=2.34$, $p=0.1053$) and during the CS period (Fig. 4f: treatment, $F_{1,30}=5.59$, $p=0.0247$; interaction, $F_{2,60}=0.24$, $p=0.7865$). In addition, CORT-treated mice traveled longer distance than Veh-treated mice during the pre-CS period (Additional file 3: Fig. S2c: treatment, $F_{1,30}=11.64$, $p=0.0019$; interaction, $F_{2,60}=3.11$, $p=0.0518$) and during the CS period (Additional file 3: Fig. S2c: treatment, $F_{1,30}=4.29$, $p=0.0470$; interaction, $F_{2,60}=0.11$, $p=0.8966$). There were no significant differences in freezing and distance traveled between the treatment groups during the pre-CS and CS periods in the cued test 28 days after the conditioning (Fig. 4h and Additional file 3: Fig. S2e). These observations suggest that chronic CORT treatment induced generalized fear and enhanced cued fear memory at least 1 day after the conditioning in CORT-treated mice, and that CORT-induced behavioral changes did not last for 4 weeks after the conditioning.

No deficits in spatial reference memory in CORT-treated mice

In the acquisition session of the Barnes maze test, there were no significant main effects of treatment and no significant treatment × time interactions on the latency to reach the target hole (Fig. 5a: treatment, $F_{1,17}=0.32$, $p=0.5781$; interaction, $F_{8,136}=0.31$, $p=0.9608$), distance traveled to reach the target hole (Fig. 5b: treatment, $F_{1,17}=0.03$, $p=0.8582$; interaction, $F_{8,136}=0.81$, $p=0.5931$), and number of errors to reach the target hole (Fig. 5c: treatment, $F_{1,17}=0.03$, $p=0.8717$; interaction, $F_{8,136}=0.88$, $p=0.5356$). In the first acquisition session, CORT-treated mice showed a significantly lower number of omissions than Veh-treated mice (Fig. 5d: treatment, $F_{1,17}=0.07$, $p=0.7953$; interaction, $F_{8,136}=2.18$, $p=0.0331$), suggesting that CORT-treated mice had increased motivation to escape from the maze.

In the probe tests conducted 1 day and 28 days after the acquisition session, there was no significant effect of treatment on time spent around the target hole between CORT- and Veh-treated mice (Fig. 5e, h: for probe test 1, $t_{17}=0.82$, $p=0.4230$; for probe test 2, $t_{17}=2.01$, $p=0.0601$). Veh-treated mice spent more time around the target hole than around the adjacent holes (Fig. 5f, i: for probe test 1, $t_{13}=5.85$, $p<0.0001$; for probe test 2, $t_{13}=2.42$, $p<0.0307$) and around the non-target holes (Fig. 5g, j: for probe test 1, $t_{13}=6.67$, $p<0.0001$; for probe test 2, $t_{13}=4.00$, $p=0.0015$). CORT-treated mice also spent a significantly longer time around the target hole than around the non-target holes in the probe test 2 (Fig. 5g, j: for probe test 1, $t_4=2.23$, $p=0.0891$; for probe test 2, $t_4=3.00$, $p=0.0398$), although there were no significant differences between the time spent around the target hole and the mean time spent around the adjacent holes (Fig. 5f, i: for probe test 1, $t_4=1.50$, $p=0.2090$; for probe test 2, $t_4=1.92$, $p=0.1275$). These results indicate that CORT-treated mice exhibited no obvious deficits in spatial reference memory.

Increased plasma CORT levels in CORT-treated mice

One-half of the mice treated with CORT or vehicle for 4 weeks were subjected to the tail suspension test to measure stress-induced levels of plasma CORT. CORT-treated mice exhibited greater immobility than Veh-treated mice (Additional file 4: Fig. S3a: $F_{1,13}=12.39$, $p=0.0038$; interaction, $F_{9,117}=0.82$, $p=0.6032$). Immediately after the test, blood was collected from the tested mice and the remaining mice that were not subjected to the test. Two-way ANOVA showed a significant main effect of treatment and no significant interaction in CORT levels (Additional file 4: Fig. S3b: treatment, $F_{1,24}=5.33$, $p=0.0299$; test, $F_{1,24}=0.39$, $p=0.5401$; interaction, $F_{1,24}=2.60$, $p=0.1197$). Post-hoc analysis indicated that CORT-treated mice had higher plasma CORT levels than Veh-treated mice, although there was no significant difference in plasma CORT levels between the two treatment groups subjected to the tail suspension test ($t_{13}=0.62$, $p=0.5469$) or between Veh-treated mice subjected to the behavioral test and CORT-treated mice that were not tested ($t_{11}=0.97$, $p=0.3510$).

Decreased weights of adrenal glands, thymus, and spleen in CORT-treated mice

After 6 weeks of treatment, CORT-treated mice had significantly lower weights of the adrenal glands (Fig. 6a: $t_{20}=6.89$, $p<0.0001$), thymus (Fig. 6b: $t_{20}=5.22$, $p<0.0001$), and spleen (Fig. 6c: $t_{20}=26.31$, $p<0.0001$) than Veh-treated mice. These data indicate CORT-induced organ atrophy.

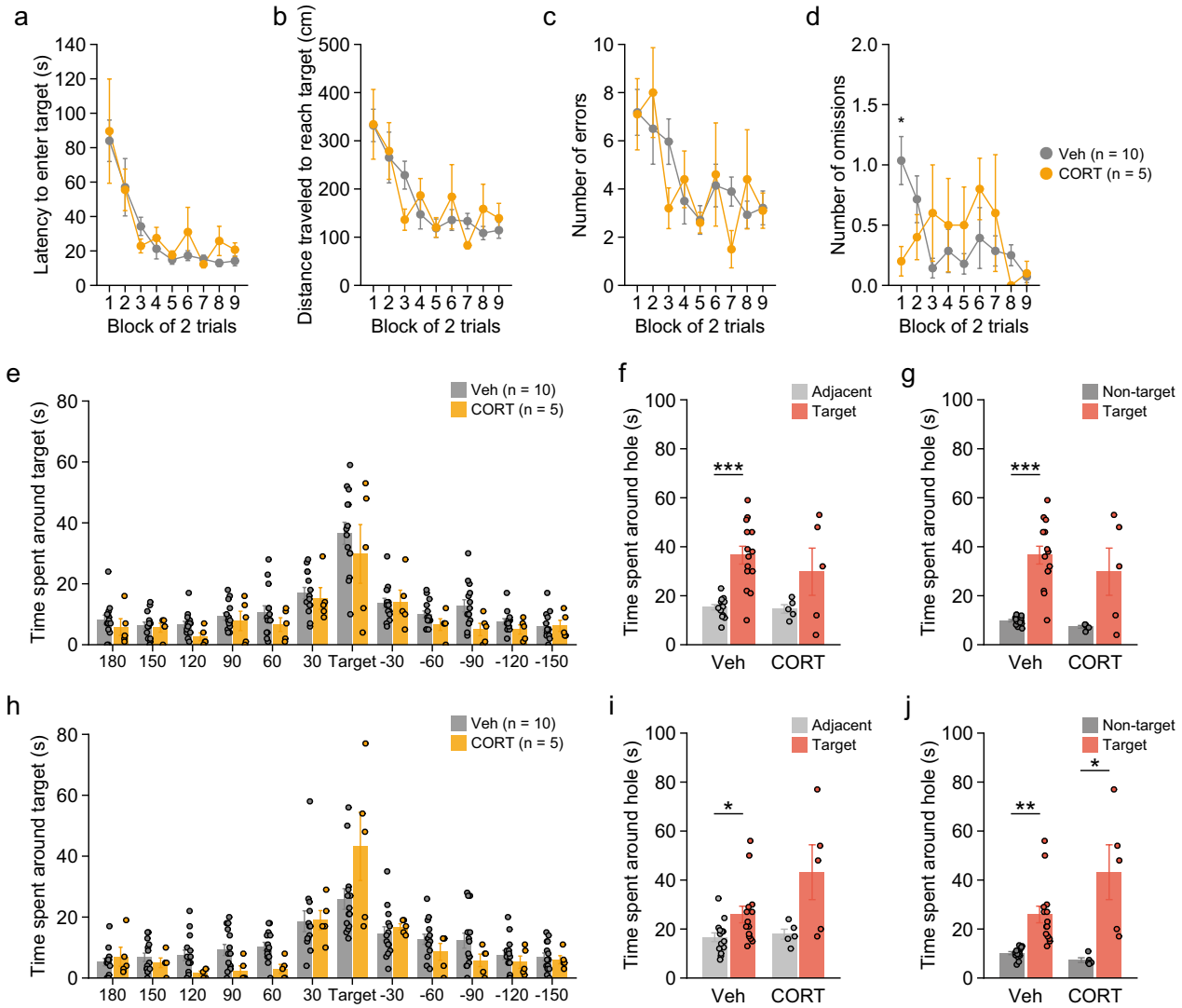

Fig. 5 Spatial memory in mice chronically treated with corticosterone. **a**–**j** Barnes maze test: **a** latency to enter the target hole (s), **b** distance traveled to first reach the target hole (s), **c** number of errors to first reach the target hole, and **d** number of omissions across the acquisition session. **e**–**g** Probe trial performed 1 day after the last acquisition session: **e** time spent around each hole (s), **f** time spent around the target and adjacent holes (s), and **g** time spent around the target and non-target holes (s). **h**–**j** Probe trial tested 28 days after the last acquisition session: **h** time spent around each hole (s), (i) time spent around the target and adjacent holes (s), and **j** time spent around the target and non-target holes (s). Values are means ± SEM. *p < 0.05. **p < 0.01. ***p < 0.001

Altered intestinal microbial composition in CORT-treated mice

The abundant microbial taxa at the phylum level were *Firmicutes*, *Bacteroidetes*, and *Actinobacteria* (taxonomies with mean relative abundance above 1% in either group and 'Others' that are taxonomies with a relative abundance of less than 1% or not identified were shown in Fig. 7a; for details, see Additional file 1: Table S5). Statistical analysis revealed that CORT-treated mice showed a higher abundance of *Actinobacteria* and *Candidatus Saccharibacteria* than Veh-treated mice (Additional file 1: Table S5: $\chi^2 = 10.59$, $p = 0.0011$; $\chi^2 = 7.08$, $p = 0.0078$, respectively). At the genus level (Fig. 7b; for details, see Additional file 1: Table S6), there were no significant differences between the two treatment groups in the measures of alpha diversity: observed number of species (Fig. 7c: $t_{14} = 0.30$, $p = 0.7668$), Chao1 index (Fig. 7d: $t_{14} = 0.87$, $p = 0.3979$), and Shannon index (Fig. 7e: $t_{14} = 1.07$, $p = 0.3044$), which indicates that CORT- and Veh-treated mice have similar species richness and evenness in fecal samples. The beta diversity representing the dissimilarity of microbial composition between the two

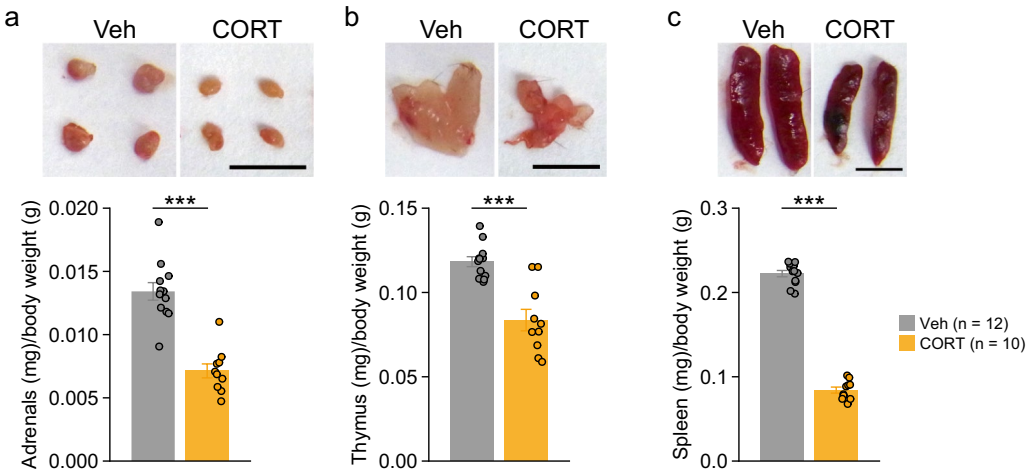

Fig. 6 Organ weights of mice chronically treated with corticosterone. **a** Adrenal gland weight (mg)/body weight (g), **b** thymus weight (mg)/body weight (g), and **c** spleen weight (mg)/body weight (g) in CORT- and Veh-treated mice. Scale bars: 5 mm. Values are means ± SEM. ***$p < 0.001$

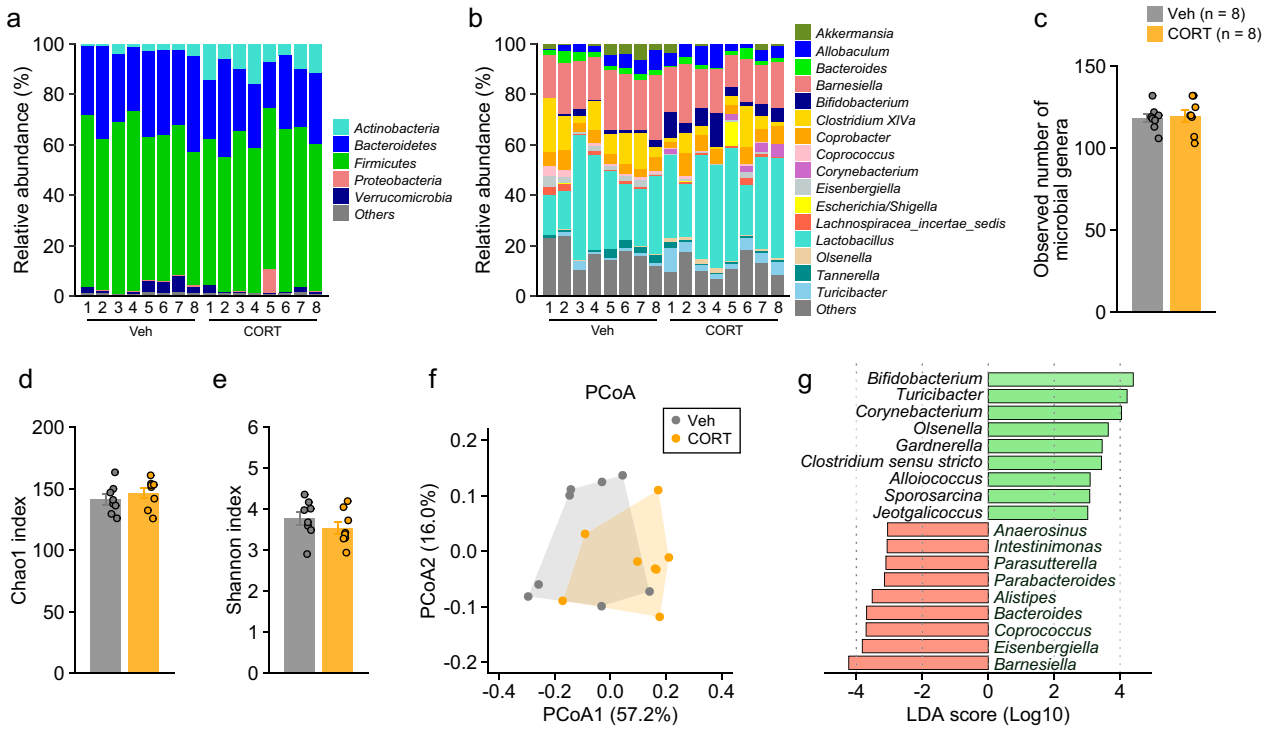

Fig. 7 Intestinal microbial composition in mice chronically treated with corticosterone. **a**, **b** Relative abundance (%) of intestinal microbiota at the phylum and genus levels in each mouse (taxonomies with a relative abundance of less than 1% or not identified were included in 'Others'). **c**–**e** Alpha diversity of the microbiota at the genus level: **c** observed number of microbial genera, **d** Chao1 index, and **e** Shannon index. **f** Beta diversity of the microbiota at the genus level was visualized using principal coordinate analysis (PCoA) with Bray–Curtis dissimilarity. **g** Taxa were differentially abundant between CORT- and Veh-treated mice (n = 8 in each group), which was identified by the linear discriminant analysis (LDA) effect size (LEfSe) method (LDA score > 3, $p < 0.05$). Values are means ± SEM

groups was visualized with principal coordinate analysis (PCoA) using Bray–Curtis dissimilarity (Fig. 7f), and permutational multivariate analysis of variance (PERMANOVA) showed significant group differences for Bray–Curtis dissimilarity ($F_{1,14} = 4.19$, $p = 0.015$). Further analysis using the linear discriminant analysis (LDA) effect size (LEfSe) method revealed that there were significant effects of treatment on 18 genera (LDA score > 3,

$p < 0.05$), indicating differences in microbial composition that CORT-treated mice had increased abundances of 9 genera (*Bifidobacterium*, *Turicibacter*, *Corynebacterium*, *Olsenella*, *Gardnerella*, *Clostridium sensu stricto*, *Alloiococcus*, *Sporosarcina*, and *Jeotgalicoccus*) and decreased abundances of 9 genera (*Barnesiella*, *Eisenbergiella*, *Coprococcus*, *Bacteroides*, *Alistipes*, *Parabacteroides*, *Parasutterella*, *Intestinimonas*, and *Anaerosinus*) compared to Veh-treated mice (Fig. 7f).

Chronic CORT treatment-induced metabolomic changes in the brain and plasma

First, we investigated the effect of chronic CORT treatment on brain neurotransmitters, which is hypothesized to be associated with depression (Fig. 8a: for statistical results of monoamines, glutamate, GABA, other neurotransmitters, and tryptophan, which is a substrate for the synthesis of serotonin, see Additional file 1: Table S7). CORT-treated mice showed decreased levels of serotonin in the CA and its metabolite 5-hydroxyindoleacetic acid (5-HIAA) in the Hb/PVT, DG, and hypothalamus (Fig. 8a: all $p < 0.05$). CORT-treated mice also exhibited decreased serotonin and 5-HIAA levels in the mPFC, although the differences did not reach a significance level (Fig. 8a and Additional file 1: Table S7: $p = 0.0585$ and $p = 0.0546$, respectively). Lower levels of tryptophan were observed in the mPFC, Hb/PVT, CA, and hypothalamus of CORT-treated mice (Fig. 8a: all $p < 0.05$). In addition, CORT-treated mice showed decreased levels of dopamine in the CA, normetanephrine in the Hb/PVT, and acetylcholine in all the brain regions, and GABA in the Hb/PVT and CA, compared to Veh-treated mice ($p < 0.05$), while increased dopamine turnover was observed in the CORT-treated mice in the CA (Fig. 8a and Additional file 1: Tables S7 and S8: $p < 0.05$). In the plasma, there were no significant differences in neurotransmission-related molecules between CORT- and Veh-treated mice (Fig. 8a).

Next, metabolomic profiles of brain regions and plasma were visualized using principal component analysis (PCA) of metabolomic data from both CORT- and Veh-treated mice (Additional file 5: Fig. S4a). The PCA plot indicates differences in the metabolomic profiles between the brain and plasma. In each brain region and plasma, a visual inspection of the metabolites using PCA plots was conducted to investigate whether the CORT-treated group was separated from the Veh-treated group. The PCA plots of each brain region and plasma showed no clear separation between the treatment groups (Fig. 8b, e, h; Additional file 5: Fig. S4b, e, and h). PLS-DA revealed different metabolic patterns between the treatment groups (Fig. 8c, f, i, and Additional file 5: Fig. S4c, f, and i). In each brain region and plasma, lists of metabolites with VIP scores (VIP > 1.0) and p value of t-test for group comparison in each metabolite ($p < 0.05$) were used for enrichment (over-representation analysis, ORA) using MetaboAnalyst 5.0 (see Additional file 1: Table S8). The enrichment analysis showed that significantly enriched metabolite sets were betaine and methionine metabolism in each brain region, as indicated by decreased levels of adenosine, choline, cystathionine, glycine, dimethylglycine, methionine, and FAD in the brain regions of CORT-treated mice (Additional file 1: Table S8), and glycine and serine metabolism and methionine metabolism in plasma (Fig. 8c, f, i and Fig. S4d, g, j).

Discussion

The present study showed that administration of CORT via drinking water for more than 4 weeks resulted in alterations across multiple aspects of behavior, including decreased locomotor activity, increased anxiety-like and depression-related behaviors, decreased social behavior in novel and familiar environments, reductions in acoustic startle response and prepulse inhibition, impaired working memory, reduced recent and remote contextual fear memory, and increased cued fear memory, but no significant changes in muscular strength and spatial reference learning and memory. Behavioral data demonstrate that mice chronically treated with CORT can be used as an animal model with high construct and face validity for studying anxiety and depression. Moreover, the current study revealed that long-term exposure to CORT leads to changes in intestinal microbial composition and metabolic shifts in both the plasma and brain. These findings imply a possible link between CORT-induced alterations in behavior and the gut–brain axis.

Basal plasma CORT levels in mice treated with CORT were comparable to those in vehicle-treated mice subjected to the tail suspension test. This suggests that the blood CORT levels induced by our oral administration regimen were equivalent to those triggered by stress in the test condition, which was designed to elicit depression-related behavior. The body weights of mice exposed to CORT by the administration regimen increased, which is consistent with the findings of previous studies [72–76]. Body weight gain is one of the physical features of depression, as observed in several mouse models of depression, such as the subchronic and mild social defeat stress model [77], chronic subordination stress model [78], postpartum depression model [55], and the SERT-deficient model [60]. Glucocorticoids induce lipolysis and proteolysis to provide energetic fuels for the stress response and contribute to fat storage and adipogenesis [79, 80], which might result in body weight gain. The increased body weight of CORT-treated mice may be partially due to hyperphagia, as indicated by their

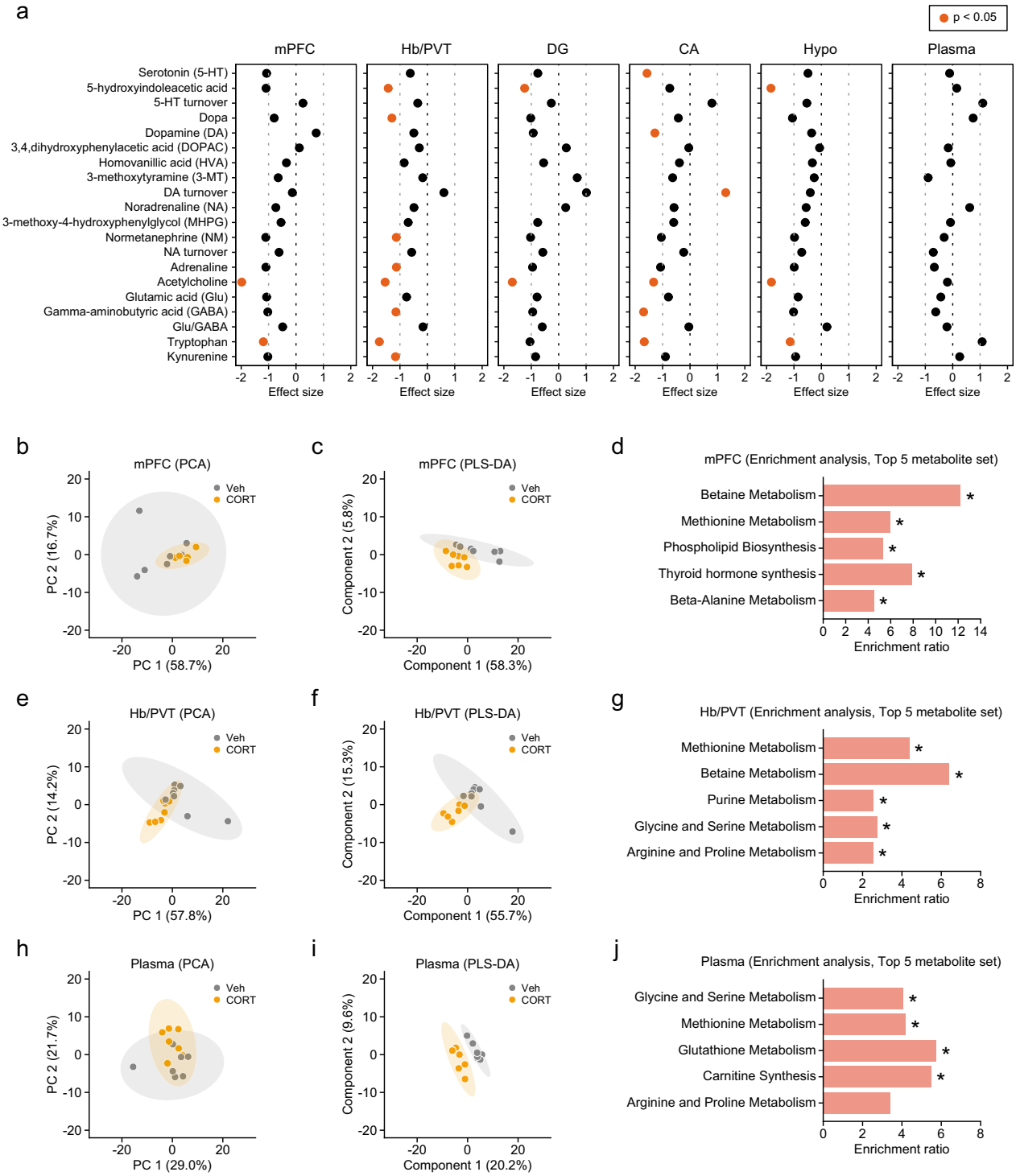

Fig. 8 Brain and plasma metabolites in mice chronically treated with corticosterone. **a** Brain and plasma metabolites related to neurotransmission in CORT- and Veh-treated mice. **b**, **e**, **h** Principal component analysis (PCA) score plots of metabolomic data in CORT- and Veh-treated mice. **c**, **f**, **i** Partial least squares discriminant analysis (PLS-DA) score plots of metabolomic data. **d**, **g**, **j** Enrichment analysis of metabolites with a VIP value of > 1 in PLS-DA and p-value of < 0.05 in the t-test for comparisons between CORT- and Veh-treated mice. **b**–**d** Medial prefrontal cortex (mPFC). **e**–**g** Habenula/paraventricular nucleus of the thalamus (Hb/PVT). **h**–**j** Plasma. *p < 0.05

increased food and solution intake. In contrast, chronic exposure to CORT caused a decrease in the weight of the immune organs (thymus, spleen, and adrenal glands), as reported in previous studies [16, 73, 82, 83]. Considering that glucocorticoids have pleiotropic effects on the immune system [3, 84], atrophy of immune organs may reflect the possibility of a compensatory mechanism to the long-term elevation of CORT levels or dysfunction of the immune system that can render mice more vulnerable to anxiety- and depression-related behaviors.

Long-term exposure to CORT resulted in decreased locomotor activity and increased anxiety-like and depression-related behaviors, which is consistent with previous findings [5–17]. A number of reports have shown that mice chronically treated with CORT exhibit reduced sucrose preference or anhedonia-like behavior [10, 75, 85–87]. Similarly, in the present study, decreased sucrose intake was observed in CORT-treated mice. The results of these studies indicate that prolonged exposure to CORT leads to behavioral consequences that seem comparable to some of the core features of depression.

Chronic CORT treatment caused a slight decrease in social contacts, reduced duration of active contacts, and increased duration per contact in a novel environment of the social interaction test, which might be attributed to decreased locomotor activity. Some reports have showed a negative association between depressive symptoms and the amount of social interactions [88, 89], although others have reported no difference in the quantity of social interactions between participants with depressive symptomatology and controls [90–92]. With our knowledge, it remains unknown whether the increased mean duration per contact is observed in depressive patients. The behavioral characteristics, i.e., reduced duration of active contacts, increased mean duration per contact, and decreased distance traveled, were seen in 5-HTT−/− mice, which are considered as an animal model for depression [60]. These findings raise the possibility that the behavioral pattern may be commonly observed among mouse models for depression. CORT-treated mice also exhibited a decreased number of physical contacts in the familiar environment of the home cage social interaction test, suggesting reduced social interaction during the light and dark phases. The result of the home cage test may not be explained by basal locomotor activity, at least during the light phase, during which CORT- and Veh-treated mice did not differ in activity levels. Given the limited number of studies, more animal and human studies are needed to validate the association of depression and the behavioral traits in a dyadic social interaction. Reduced social behavior in CORT-treated mice has been reported in previous studies using the three-chamber sociability test and in the social interaction test adopted in the social defeat paradigm [75, 86, 93–95]. Consistent with previous reports in which social behavior was measured over a short period, that is, for 2.5 or 5 min, the present study indicates reduced social preference in CORT-treated mice during the first 5-min period of the sociability test. Our study further revealed no apparent impairment in social memory assessed using the social novelty preference test in the three-chamber paradigm. These findings suggest that long-term exposure to CORT disrupts the social approach in novel and familiar environments but causes no apparent deficits in social recognition memory.

Chronic administration of CORT induced cognitive deficits in a variety of behavioral paradigms for working memory in the Y-maze test [94–96], spatial memory in the Morris water maze test [97–100] and the Barnes maze test [97], and fear memory in the step-down and step-through passive avoidance test [95, 98, 101–105] and fear conditioning test [97, 106]. The Y-maze test has been conducted using a continuous trials procedure that allowed the animals to freely explore the three arms of the Y-maze [94–96]. The Y-maze continuous procedure has the possibility of inter-trial interference that may cause modest spontaneous alternation rates [107]. Additionally, if an animal has a side preference (e.g., always turning right) in the Y-maze, this will result in high alternation rates [107]. Thus, the continuous procedure can complicate the interpretation of behavioral consequences. The T-maze test used in the present study consisted of a forced-choice run followed by a free-choice run in each trial, with an inter-trial interval of 60 s, possibly reducing the influence of inter-trial interference. Our T-maze test results confirmed that chronic CORT treatment caused working memory deficits.

In contrast to a previous study [97], our study failed to find any significant behavioral differences between CORT- and Veh-treated mice in the Barnes maze test. The acquisition of spatial memory in the Barnes maze task with a large number of holes is considered difficult [108]. The maze apparatus utilized in a prior study by Darcet et al. [97] possessed a higher number of holes (20 in total) than that employed in the current study (12 holes), which might enable the former study to detect behavioral differences between the treatment groups. In the present study, a lower number of omissions to enter the escape box in the first acquisition session was observed in CORT-treated mice, suggesting that chronic CORT treatment increases the motivation to escape from the open space illuminated by bright lights. This aversive motivation might have contributed to the lack of deficits in the reference memory of CORT-treated mice, as demonstrated in this study.

CORT-treated mice exhibited decreased freezing in the context test and increased freezing in the cued test 1 day after conditioning, which is consistent with previous reports [97, 106]. The reduced freezing in the same context as that during conditioning may be explained by impaired reactivation and retrieval of contextual memory and/or increased escape responses to the conditioning context due to heightened fear in CORT-treated mice. Increased freezing during the pre-CS period of the cued test was context-independent, suggesting increased generalized fear in CORT-treated mice. Although the results of freezing in the context and cued tests appear to be somewhat contradictory, these findings may support the conclusion that long-term exposure to CORT is associated with an increase in fear responses. About 1 month after conditioning, CORT-treated mice displayed reduced freezing behavior during the context test, and there were no differences in freezing between CORT- and Veh-treated mice during the cued test. These results suggest impairments in long-term or remote fear memory in CORT-treated mice. Taken together, our data indicate that long-term exposure to CORT leads to various behavioral disturbances, including increased anxiety- and depression-like behaviors, reduced social behavior, and cognitive dysfunction, indicating that CORT-treated mice are a valid animal model for studying anxiety and depression.

Increasing evidence has shown that altered composition of the gut microbiota is associated with depression through the gut microbiota–brain axis [109–111]. In the present study, chronic CORT treatment induced changes in fecal microbial composition, as indicated by the increased abundance of the phyla *Actinobacteria* and *Candidatus Saccharibacteria* (formerly known as *TM7*) in the feces of CORT-treated mice, consistent with the findings of a recent study showing a similar trend for the two phyla in the cecal contents of CORT-treated mice [31]. Previous studies have reported that CORT-treated mice had an increased abundance of the phylum *Firmicutes* and a decreased abundance of the phylum *Bacteroidetes* in cecal contents [30, 31]. In our study, although CORT-treated mice exhibited a tendency toward a decrease in the abundance of *Bacteroidetes* compared to Veh-treated mice, no significant difference in the abundance of *Firmicutes* was observed between the treatment groups. These seemingly inconsistent results may be due to methodological differences in sampling sites (cecal contexts in previous studies and feces in the present study) and environmental conditions [112, 113] between the studies.

Our study further revealed differences in fecal microbiota at a more detailed taxonomic or genus level between CORT- and Veh-treated groups, as indicated by the increased abundance of *Bifidobacterium*, *Turicibacter*, *Corynebacterium*, and *Olsenella* and the decreased abundance of *Barnesiella*, *Eisenbergiella*, *Coprococcus*, *Bacteroides*, and *Alistipes* in CORT-treated mice. An increase or decrease in the abundance of *Bifidobacterium* has been observed in individuals with major depressive disorder [114, 115] and in stress-induced mouse models of depression [116, 117]. Some studies have indicated that the administration of *Bifidobacterium* species has beneficial and antidepressant effects [118, 119] and attenuates stress-induced increases in CORT levels [120, 121]; the increased abundance of *Bifidobacterium* may serve as a compensatory mechanism to counteract the behavioral and physiological effects of chronic CORT administration. The altered gut microbial composition caused by chronic exposure to CORT is partially similar to that observed in individuals with depression, as indicated by the increased abundance of *Olsenella* and decreased abundance of *Alistipes* and *Coprococcus* [115, 122–125]. In contrast to the microbial composition of CORT-treated mice, decreased abundance of *Corynebacterium* and increased abundance of *Eisenbergiella* were found in some animal models of chronic stress-induced depression [126–128], while decreased abundance of *Turicibacter* and increased abundance of *Barnesiella* and *Bacteroides* were observed in individuals with depression [115, 123, 125, 129, 130]. *Turicibacter* and *Corynebacterium* have been reported to increase or decrease in inflammatory bowel disease models [131–133] and diet-induced obesity models [134–137], suggesting that they can act as mediators of both pro-inflammatory and anti-inflammatory effects. Accumulating evidence indicates that increased activity in the immune system and inflammatory processes contribute to the development of depression [138–140] and that anti-inflammatory agents, including glucocorticoids, have antidepressant properties [139, 141]. These findings imply that chronic CORT-induced changes in the abundance of these genera, similar to *Bifidobacterium*, may be involved in the compensatory mechanism to inflammatory-related conditions, although the underlying mechanisms remain unknown. In this study, fecal microbiome was determined at the time point of 5 weeks following CORT exposure. Gut microbial composition can be affected by various environmental factors [32]. Thus, it is important to further explore the changes in gut microbial composition across different time points before and after CORT exposure under different environments to draw reliable conclusions regarding CORT-induced changes in gut microbiota. In addition, and further research is needed to clarify the precise role of the genera changed by elevated CORT conditions in behavioral and brain functions.

Our metabolic analysis revealed alterations in plasma glycine and serine metabolism, such as decreased glycine levels in CORT-treated mice. Glycine deficiency is associated with obesity and metabolic diseases [142]. Several studies have reported altered blood glycine levels in patients with depression, although the results have been inconsistent [143–146]. Glycine is degraded in the intestine by microbiota [147, 148]. Administration of *Lactobacillus paracasei* to the gut of germ-free mice results in decreased levels of glycine in the intestine [149]. These findings suggest that the peripheral metabolomic changes induced by CORT exposure could be mediated by alterations in gut microbial composition.

The present study showed decreased serotonin and 5-HIAA levels, accompanied by reduced tryptophan levels, in almost all brain regions in CORT-treated mice. CORT-treated mice also showed lower levels of dopamine, normetanephrine, and GABA in some brain regions. Decreased levels of neurotransmitters and their metabolites suggest chronic CORT-induced dysfunction in serotonergic, dopaminergic, noradrenergic, and GABAergic neurotransmission in the brain, which is consistent with the monoaminergic and GABAergic deficit hypothesis of depression [40, 150, 151]. Acetylcholine and monoamines in the brain contribute to attention, working memory, and other cognitive functions [152, 153]. Chronic CORT treatment decreased choline and acetylcholine levels in all the brain regions examined, which might be associated with impairments in PPI, fear memory, and working memory.

Enrichment analysis of the metabolomic data revealed alterations in betaine, methionine, and glycine metabolism induced by chronic CORT treatment in the brain, as indicated by decreased levels of choline, dimethylglycine, methionine, and glycine, which are commonly observed in the brain regions examined. Choline can be metabolized to betaine, which converts homocysteine to methionine, generating dimethylglycine metabolized to glycine, which is suggested to be an important nutrient for the prevention of chronic diseases and psychiatric disorders [154–157]. *S*-Adenosyl-methionine (SAMe), formed from methionine, has been used to treat depression [158]. In the present study, brain and plasma SAMe levels in CORT-treated mice were similar to those in Veh-treated mice. These results suggest that choline and methionine might be highly metabolized to maintain a normal level of SAMe in CORT-treated mice. Betaine improves the antidepressant effect of SAMe in patients with depression [159] and exerts an antidepressant effect in animal models of depression [160, 161]. Although this study did not measure betaine itself, the reduced metabolites of the betaine and methionine pathways suggest the possibility of betaine deficiency in CORT-treated mice. Consistent with a recent systematic review of metabolomic studies in animal models of depression, such as the chronic mild stress model, social defeat model, and LPS model [34], our findings suggest that decreased levels of metabolites for betaine and methionine metabolism as well as neurotransmission in the brain may be associated with a depressive state induced by chronic CORT exposure.

Accumulating evidence suggests that the gut microbiota can influence various nervous system functions via host metabolism, immune response, and neurotransmission [20, 25, 162]. Our study showed that chronic CORT treatment induced altered fecal microbial composition and plasma and brain metabolomic changes, which were accompanied by changes in a wide range of behaviors such as increased anxiety-like and depression-related behaviors, decreased social behavior, and disrupted working and fear memory. These findings suggest an association between gut microbial and metabolomic changes induced by CORT exposure and behavioral consequences relevant to depression. Some limitations should be taken into account in this study. First, ethanol solution was used as the vehicle. Ethanol consumption could affect basal levels of behavior, gut microbiota, and metabolites, which might mask or enhance the effects of corticosterone. Second, there is a lack of data on fecal metabolites. Fecal metabolome provides a functional readout of the gut microbiota [163], which could help us understand the relationship between CORT-induced changes in gut microbiota and plasma and brain metabolites. Third, our study did not include females. Sex differences in depression have been documented in humans, and its prevalence is twofold higher in women than in men [164, 165]. The use of both male and female animals is needed to comprehensively understand the effects of CORT exposure in the research of depression model. Finally, gut microbial analysis and metabolomics analysis were done using different cohorts of mice. Therefore, analysis of correlations between gut microbiota, metabolites, and behavior could not be performed to determine the relationship between the CORT-induced changes. Although further investigation is needed to reveal the causal link between chronic CORT-induced changes in the gut microbiota, metabolites, and behaviors, the findings of the present study provides important clues about the development of depression and potential targets for its treatment.

Supplementary Information

The online version contains supplementary material available at https://doi.org/10.1186/s13041-024-01146-x.

Additional file 1: Supplementary Table 1. A battery of behavioral tests in mice chronically treated with corticosterone. Supplementary Table 2. The weight of brain tissue used for metabolomic analysis. Supplementary

Table 3. The Q1 or Q3 pre bias voltages, collision energies and mass transitions used in metabolomic analysis. Supplementary Table 4. Statistical analysis of behavioral data in mice chronically treated with corticosterone. Supplementary Table 5. Relative abundance of the intestinal microbiota at the phylum level in mice chronically treated with corticosterone. Supplementary Table 6. Relative abundance of the intestinal microbiota at the genus level in mice chronically treated with corticosterone. Supplementary Table 7. Neurotransmitters and their metabolites in the plasma and brain of mice chronically treated with corticosterone. Supplementary Table 8. Brain and plasma metabolites in mice chronically treated with corticosterone

Additional file 2: Supplementary Figure 1. Body weight and food and solution intake in mice chronically treated with corticosterone. **a** Body weight of mice treated with CORT for 12 weeks. **b** Mean food intake per mouse per day during the 8-week treatment period. **c** Mean solution intake per mouse per day during the 8-week treatment period. Values are means ± SEM. ***$p < 0.001$

Additional file 3: Supplementary Figure 2. Behavior in mice chronically treated with corticosterone. **a–e** Distance traveled in the fear conditioning test: **a** conditioning session on day 1, **b** context test on day 2, **c** cued test on day 2, **d** context test on day 29, and **e** cued test on day 29. **f–h** Distance traveled before, during, and after exposure to the first, second, and third US for 6 s in the conditioning session of the fear conditioning test. Values are means ± SEM. *$p < 0.05$

Additional file 4: Supplementary Figure 3. Plasma CORT levels in mice chronically treated with corticosterone. Approximately half of the CORT- and Veh-treated mice were subjected to the tail suspension test. The remaining half of the mice were left undisturbed in their home cages. **a** Percentage of immobility time in the TS test. **b** CORT levels in plasma taken from CORT- and Veh-treated mice that were either subjected to the TS or left undisturbed in HC. Values are means ± SEM. *$p < 0.05$. *$p < 0.01$

Additional file 5: Supplementary Figure 4. Brain metabolites in mice chronically treated with corticosterone. **a** Principal component analysis score plot of metabolomic data from the plasma and brain. **b, e, h** PCA score plots of metabolomic data from CORT- and Veh-treated mice. **c, f, i** Partial least squares discriminant analysis score plot of metabolomic data. **d, g, j** Enrichment analysis of metabolites with a VIP value of > 1 in PLS-DA and p-value of < 0.05 in the t-test for comparisons between CORT- and Veh-treated mice. **b–d** Dentate gyrus. **e–g** CA in the hippocampus. **h–j** Hypothalamus. *$p < 0.05$

Acknowledgements
We would like to thank Tamaki Murakami and Harumi Mitsuya for their assistance in animal husbandry, behavioral experiments, and preparation of this paper. Behavioral analysis was carried out at the Joint Usage/Research Center for Genes, Brain and Behavior in the Center for Medical Science at Fujita Health University, which is accredited by the Ministry of Education, Science, Sports and Culture of Japan.

Author contributions
HS performed experiments, analyzed the data, and wrote the manuscript. YM performed metabolomic analysis. TM coordinated the study, interpreted data, and wrote the manuscript. All authors have read and approved the final manuscript.

Funding
This study was supported by AMED (Grant Number JP21dm0107101), JSPS KAKENHI (Grant Number JP21K03151), and MEXT Promotion of Distinctive Joint Research Center Program (Grant Numbers FY2018-2020 JPMXP0618217663 and FY2021-2023 JPMXP0621467949).

Availability of data and materials
All the data used in this study are available from the authors upon request.

Declarations

Ethics approval and consent to participate
All experimental procedures were approved by the Institutional Animal Care and Use Committee of Fujita Health University.

Consent for publication
Not applicable.

Competing interests
The authors declare that they have no competing interests.

Received: 22 June 2024 Accepted: 26 September 2024
Published online: 07 November 2024

References

1. Erickson K, Drevets W, Schulkin J. Glucocorticoid regulation of diverse cognitive functions in normal and pathological emotional states. Neurosci Biobehav Rev. 2003;27(3):233–46.
2. Vegiopoulos A, Herzig S. Glucocorticoids, metabolism and metabolic diseases. Mol Cell Endocrinol. 2007;275(1–2):43–61.
3. Cain DW, Cidlowski JA. Immune regulation by glucocorticoids. Nat Rev Immunol. 2017;17(4):233–47.
4. Pariante CM, Lightman SL. The HPA axis in major depression: classical theories and new developments. Trends Neurosci. 2008;31(9):464–8.
5. Wang G, Cheng Y, Gong M, Liang B, Zhang M, Chen Y, Zhang C, Yuan X, Xu J. Systematic correlation between spine plasticity and the anxiety/depression-like phenotype induced by corticosterone in mice. NeuroReport. 2013;24(12):682–7.
6. Brachman RA, McGowan JC, Perusini JN, Lim SC, Pham TH, Faye C, Gardier AM, Mendez-David I, David DJ, Hen R, Denny CA. Ketamine as a prophylactic against stress-induced depressive-like behavior. Biol Psychiatry. 2016;79(9):776–86.
7. Ibi M, Liu J, Arakawa N, Kitaoka S, Kawaji A, Matsuda KI, Iwata K, Matsumoto M, Katsuyama M, Zhu K, Teramukai S, Furuyashiki T, Yabe-Nishimura C. Depressive-like behaviors are regulated by NOX1/NADPH oxidase by redox modification of NMDA receptor 1. J Neurosci. 2017;37(15):4200–12.
8. Luo GQ, Liu L, Gao QW, Wu XN, Xiang W, Deng WT. Mangiferin prevents corticosterone-induced behavioural deficits via alleviation of oxido-nitrosative stress and down-regulation of indoleamine 2, 3-dioxygenase (IDO) activity. Neurol Res. 2017;39(8):709–18.
9. Mendez-David I, Boursier C, Domergue V, Colle R, Falissard B, Corruble E, Gardier AM, Guilloux JP, David DJ. Differential peripheral proteomic biosignature of fluoxetine response in a mouse model of anxiety/depression. Front Cell Neurosci. 2017;11:237.
10. Wang Y, Gu N, Duan T, Kesner P, Blaskovits F, Liu J, Lu Y, Tong L, Gao F, Harris C, Mackie K, Li J, Tan Q, Hill MN, Yuan Z, Zhang X. Monoacylglycerol lipase inhibitors produce pro-or antidepressant responses via hippocampal CA1 GABAergic synapses. Mol Psychiatry. 2017;22(2):215–26.
11. Sun X, Li X, Pan R, Xu Y, Wang Q, Song M. Total Saikosaponins of *Bupleurum yinchowense* reduces depressive, anxiety-like behavior and increases synaptic proteins expression in chronic corticosterine-treated mice. BMC Complement Altern Med. 2018;18(1):1–10.
12. Dieterich A, Srivastava P, Sharif A, Stech K, Floeder J, Yohn SE, Samuels BA. Chronic corticosterone administration induces negative valence and impairs positive valence behaviors in mice. Transl Psychiatry. 2019;9(1):1–13.
13. Morgan A, Kondev V, Bedse G, Baldi R, Marcus D, Patel S. Cyclooxygenase-2 inhibition reduces anxiety-like behavior and normalizes enhanced amygdala glutamatergic transmission following chronic oral corticosterone treatment. Neurobiol Stress. 2019;11: 100190.
14. Cabeza L, Ramadan B, Giustiniani J, Houdayer C, Pellequer Y, Gabriel D, Fauconnet S, Haffen E, Risold PY, Fellmann D, Belin D, Peterschmitt Y. Chronic exposure to glucocorticoids induces suboptimal decision-making in mice. Eur Neuropsychopharmacol. 2021;46:56–67.

15. Peritore AF, Crupi R, Scuto M, Gugliandolo E, Siracusa R, Impellizzeri D, Cordaro M, D'amico R, Fusco R, Paola RD, Cuzzocrea S, Cuzzocrea S. The role of annexin A1 and formyl peptide receptor 2/3 signaling in chronic corticosterone-induced depression-like behaviors and impairment in hippocampal-dependent memory. CNS Neurol Disord Drug Targets. 2020;19(1):27–43.
16. Caradonna SG, Einhorn NR, Saudagar V, Khalil H, Petty GH, Lihagen A, LeFloch C, Lee FS, Akil H, Guidotti A, McEwen BS, Gatta E, Marrocco J. Corticosterone induces discrete epigenetic signatures in the dorsal and ventral hippocampus that depend upon sex and genotype: focus on methylated Nr3c1 gene. Transl Psychiatry. 2022;12(1):1–12.
17. Gao C, Wu M, Du Q, Deng J, Shen J. Naringin mediates adult hippocampal neurogenesis and exerts antidepressant effects via activating CREB signaling. Front Cell Dev Biol. 2022. https://doi.org/10.3389/fcell.2022.731831.
18. Hooper LV, Littman DR, Macpherson AJ. Interactions between the microbiota and the immune system. Science. 2012;336(6086):1268–73.
19. O'Mahony SM, Clarke G, Borre YE, Dinan TG, Cryan JF. Serotonin, tryptophan metabolism and the brain–gut–microbiome axis. Behav Brain Res. 2015;277:32–48.
20. Fung TC, Olson CA, Hsiao EY. Interactions between the microbiota, immune and nervous systems in health and disease. Nat Neurosci. 2017;20(2):145–55.
21. Huang F, Wu X. Brain neurotransmitter modulation by gut microbiota in anxiety and depression. Front Cell Dev Biol. 2021;9: 649103.
22. Sudo N, Chida Y, Aiba Y, Sonoda J, Oyama N, Yu XN, Kubo C, Koga Y. Postnatal microbial colonization programs the hypothalamic–pituitary–adrenal system for stress response in mice. J Physiol. 2004;558(1):263–75.
23. Neufeld KM, Kang N, Bienenstock J, Foster JA. Reduced anxiety-like behavior and central neurochemical change in germ-free mice. Neurogastroenterol Motil. 2011;23(3):255–64.
24. Heijtz RD, Wang S, Anuar F, Qian Y, Björkholm B, Samuelsson A, Heijtz RD, Wang S, Anuar F, Qian Y, Björkholm B, Samuelsson A, Hibberd ML, Forssberg H, Pettersson S. Normal gut microbiota modulates brain development and behavior. Proc Natl Acad Sci USA. 2011;108(7):3047–52.
25. Foster JA, Neufeld KAM. Gut–brain axis: how the microbiome influences anxiety and depression. Trends Neurosci. 2013;36(5):305–12.
26. Luo Y, Zeng B, Zeng LI, Du X, Li BO, Huo R, Luo Y, Zeng B, Zeng L, Du X, Li B, Huo R, Liu L, Wang H, Dong M, Pan J, Zheng P, Zhou C, Wei H, Xie P. Gut microbiota regulates mouse behaviors through glucocorticoid receptor pathway genes in the hippocampus. Transl Psychiatry. 2018;8(1):1–10.
27. Rieder R, Wisniewski PJ, Alderman BL, Campbell SC. Microbes and mental health: a review. Brain Behav Immunity. 2017;66:9–17.
28. Bailey MT, Dowd SE, Galley JD, Hufnagle AR, Allen RG, Lyte M. Exposure to a social stressor alters the structure of the intestinal microbiota: implications for stressor-induced immunomodulation. Brain Behav Immun. 2011;25(3):397–407.
29. Wu M, Tian T, Mao Q, Zou T, Zhou CJ, Xie J, Chen JJ. Associations between disordered gut microbiota and changes of neurotransmitters and short-chain fatty acids in depressed mice. Transl Psychiatry. 2020;10(1):1–10.
30. Xie X, Xiao Q, Xiong Z, Yu C, Zhou J, Fu Z. Crocin-I ameliorates the disruption of lipid metabolism and dysbiosis of the gut microbiota induced by chronic corticosterone in mice. Food Function. 2019;10(10):6779–91.
31. Angoa-Pérez M, Zagorac B, Francescutti DM, Theis KR, Kuhn DM. Responses to chronic corticosterone on brain glucocorticoid receptors, adrenal gland, and gut microbiota in mice lacking neuronal serotonin. Brain Res. 2021;1751: 147190.
32. Laukens D, Brinkman BM, Raes J, De Vos M, Vandenabeele P. Heterogeneity of the gut microbiome in mice: guidelines for optimizing experimental design. FEMS Microbiol Rev. 2016;40(1):117–32.
33. Parker KD, Albeke SE, Gigley JP, Goldstein AM, Ward NL. Microbiome composition in both wild-type and disease model mice is heavily influenced by mouse facility. Front Microbiol. 2018;9:1598.
34. Pu J, Liu Y, Gui S, Tian L, Yu Y, Song X, Zhong X, Chen X, Chen W, Zheng P, Zhang H, Gong X, Liu K, Wu J, Wang H, Xie P. Metabolomic changes in animal models of depression: a systematic analysis. Mol Psychiatry. 2021;26(12):7328–36.
35. Gong MJ, Han B, Wang SM, Liang SW, Zou ZJ. Icariin reverses corticosterone-induced depression-like behavior, decrease in hippocampal brain-derived neurotrophic factor (BDNF) and metabolic network disturbances revealed by NMR-based metabonomics in rats. J Pharm Biomed Anal. 2016;123:63–73.
36. Krishnan V, Nestler EJ. The molecular neurobiology of depression. Nature. 2008;455(7215):894–902.
37. Proulx CD, Hikosaka O, Malinow R. Reward processing by the lateral habenula in normal and depressive behaviors. Nat Neurosci. 2014;17(9):1146–52.
38. Browne CA, Hammack R, Lucki I. Dysregulation of the lateral habenula in major depressive disorder. Front Synaptic Neurosci. 2018;10:46.
39. Barson JR, Mack NR, Gao WJ. The paraventricular nucleus of the thalamus is an important node in the emotional processing network. Front Behav Neurosci. 2020;14: 598469.
40. Hirschfeld RM. History and evolution of the monoamine hypothesis of depression. J Clin Psychiatry. 2000;61(6):4–6.
41. Bansal Y, Kuhad A. Mitochondrial dysfunction in depression. Curr Neuropharmacol. 2016;14(6):610–8.
42. Miller AH, Raison CL. The role of inflammation in depression: from evolutionary imperative to modern treatment target. Nat Rev Immunol. 2016;16(1):22–34.
43. Page CE, Coutellier L. Prefrontal excitatory/inhibitory balance in stress and emotional disorders: evidence for over-inhibition. Neurosci Biobehav Rev. 2019;105:39–51.
44. Shoji H, Miyakawa T. Age-related behavioral changes from young to old age in male mice of a C57BL/6J strain maintained under a genetic stability program. Neuropsychopharmacol Rep. 2019;39(2):100–18.
45. Shoji H, Miyakawa T. Differential effects of stress exposure via two types of restraint apparatuses on behavior and plasma corticosterone level in inbred male BALB/cAJcl mice. Neuropsychopharmacol Rep. 2020;40(1):73–84.
46. Crawley J, Goodwin FK. Preliminary report of a simple animal behavior model for the anxiolytic effects of benzodiazepines. Pharmacol Biochem Behav. 1980;13(2):167–70.
47. Takao K, Miyakawa T. Light/dark transition test for mice. J Vis Exp. 2006;1: e104.
48. Lister RG. The use of a plus-maze to measure anxiety in the mouse. Psychopharmacology. 1987;92(2):180–5.
49. Komada M, Takao K, Miyakawa T. Elevated plus maze for mice. J Vis Exp. 2008;22: e1088.
50. Shoji H, Miyakawa T. Effects of test experience, closed-arm wall color, and illumination level on behavior and plasma corticosterone response in an elevated plus maze in male C57BL/6J mice: a challenge against conventional interpretation of the test. Mol Brain. 2021;14(1):1–12.
51. Moy SS, Nadler JJ, Perez A, Barbaro RP, Johns JM, Magnuson TR, Piven J, Crawley JN. Sociability and preference for social novelty in five inbred strains: an approach to assess autistic-like behavior in mice. Genes Brain Behav. 2004;3(5):287–302.
52. Shoji H, Miyakawa T. Relationships between the acoustic startle response and prepulse inhibition in C57BL/6J mice: a large-scale meta-analytic study. Mol Brain. 2018;11(1):1–9.
53. Porsolt RD, Bertin A, Jalfre MJAIP. Behavioral despair in mice: a primary screening test for antidepressants. Arch Int Pharmacodyn Ther. 1977;229(2):327–36.
54. Nakao A, Miki T, Shoji H, Nishi M, Takeshima H, Miyakawa T, Mori Y. Comprehensive behavioral analysis of voltage-gated calcium channel beta-anchoring and-regulatory protein knockout mice. Front Behav Neurosci. 2015;9:141.
55. Shoji H, Miyakawa T. Increased depression-related behavior during the postpartum period in inbred BALB/c and C57BL/6 strains. Mol Brain. 2019;12(1):1–20.
56. Shoji H, Hagihara H, Takao K, Hattori S, Miyakawa T. T-maze forced alternation and left-right discrimination tasks for assessing working and reference memory in mice. J Vis Exp. 2012;60: e3300.
57. Steru L, Chermat R, Thierry B, Simon P. The tail suspension test: a new method for screening antidepressants in mice. Psychopharmacology. 1985;85(3):367–70.

58. Shoji H, Takao K, Hattori S, Miyakawa T. Contextual and cued fear conditioning test using a video analyzing system in mice. J Vis Exp. 2014;85: e50871.
59. Barnes CA. Memory deficits associated with senescence: a neurophysiological and behavioral study in the rat. J Comp Physiol Psychol. 1979;93(1):74.
60. Shoji H, Ikeda K, Miyakawa T. Behavioral phenotype, intestinal microbiome, and brain neuronal activity of male serotonin transporter knockout mice. Mol Brain. 2023;16(1):32.
61. Takao K, Shoji H, Hattori S, Miyakawa T. Cohort removal induces changes in body temperature, pain sensitivity, and anxiety-like behavior. Front Behav Neurosci. 2016;10:99.
62. Takahashi S, Tomita J, Nishioka K, Hisada T, Nishijima M. Development of a prokaryotic universal primer for simultaneous analysis of Bacteria and Archaea using next-generation sequencing. PLoS ONE. 2014;9(8): e105592.
63. Hisada T, Endoh K, Kuriki K. Inter-and intra-individual variations in seasonal and daily stabilities of the human gut microbiota in Japanese. Arch Microbiol. 2015;197:919–34.
64. Aronesty E. Comparison of sequencing utility programs. Open Bioinform J. 2013;7:1–8.
65. Gordon A, Hannon GJ. Fastx-toolkit. FASTQ/A short-reads pre-processing tools. 2010. http://hannonlab.cshl.edu/fastx_toolkit/index.html.
66. Caporaso JG, Kuczynski J, Stombaugh J, Bittinger K, Bushman FD, Costello EK, Fierer N, Peña AG, Goodrich JK, Gordon JI, Huttley GA, Kelley ST, Knights D, Koenig JE, Ley RE, Lozupone CA, McDonald D, Muegge BD, Pirrung M, Reeder J, Sevinsky JR, Turnbaugh PJ, Walters WA, Widmann J, Yatsunenko T, Zaneveld J, Knight R. QIIME allows analysis of high-throughput community sequencing data. Nat Methods. 2010;7(5):335–6.
67. Edgar RC, Haas BJ, Clemente JC, Quince C, Knight R. UCHIME improves sensitivity and speed of chimera detection. Bioinformatics. 2011;27(16):2194–200.
68. Wang Q, Garrity GM, Tiedje JM, Cole JR. Naive Bayesian classifier for rapid assignment of rRNA sequences into the new bacterial taxonomy. Appl Environ Microbiol. 2007;73(16):5261–7.
69. Oksanen J, Blanchet FG, Friendly M, Kindt R, Legendre P, McGlinn D, Minchin PR, O'Hara RB, Simpson GL, Solymos P, Stevens MHH, Szoecs E, Wagner H. Vegan: community ecology package (version 2.5-6). 2019. http://www.cran.r-project.org/package=vegan.
70. Segata N, Izard J, Waldron L, Gevers D, Miropolsky L, Garrett WS, Huttenhower C. Metagenomic biomarker discovery and explanation. Genome Biol. 2011;12(6):1–18.
71. Pang Z, Chong J, Zhou G, de Lima Morais DA, Chang L, Barrette M, Pang Z, Chong J, Zhou G, de Lima Morais DA, Chang L, Barrette M, Gauthier C, Jacques PÉ, Li S, Xia J. MetaboAnalyst 5.0: narrowing the gap between raw spectra and functional insights. Nucleic Acids Res. 2021;49(W1):W388–96.
72. Crupi R, Mazzon E, Marino A, La Spada G, Bramanti P, Cuzzocrea S, Spina E. Melatonin treatment mimics the antidepressant action in chronic corticosterone-treated mice. J Pineal Res. 2010;49(2):123–9.
73. Karatsoreos IN, Bhagat SM, Bowles NP, Weil ZM, Pfaff DW, McEwen BS. Endocrine and physiological changes in response to chronic corticosterone: a potential model of the metabolic syndrome in mouse. Endocrinology. 2010;151(5):2117–27.
74. van Donkelaar EL, Vaessen KR, Pawluski JL, Sierksma AS, Blokland A, Canete R, Steinbusch HW. Long-term corticosterone exposure decreases insulin sensitivity and induces depressive-like behaviour in the C57BL/6NCrl mouse. PLoS ONE. 2014;9(10): e106960.
75. Nicolas S, Debayle D, Béchade C, Maroteaux L, Gay AS, Bayer P, Nicolas S, Debayle D, Béchade C, Maroteaux L, Gay AS, Bayer P, Heurteaux C, Guyon A, Chabry J. Adiporon, an adiponectin receptor agonist acts as an antidepressant and metabolic regulator in a mouse model of depression. Transl Psychiatry. 2018;8(1):1–11.
76. Burtscher J, Copin JC, Rodrigues J, Kumar ST, Chiki A, de Suduiraut IG, Burtscher J, Copin JC, Rodrigues J, Kumar ST, Chiki A, de Suduiraut IG, Sandi C, Lashuel HA. Chronic corticosterone aggravates behavioral and neuronal symptomatology in a mouse model of alpha-synuclein pathology. Neurobiol Aging. 2019;83:11–20.
77. Goto T, Kubota Y, Tanaka Y, Iio W, Moriya N, Toyoda A. Subchronic and mild social defeat stress accelerates food intake and body weight gain with polydipsia-like features in mice. Behav Brain Res. 2014;270:339–48.
78. Dadomo H, Sanghez V, Di Cristo L, Lori A, Ceresini G, Malinge I, Parmigiani S, Palanza P, Sheardown M, Bartolomucci A. Vulnerability to chronic subordination stress-induced depression-like disorders in adult 129SvEv male mice. Prog Neuropsychopharmacol Biol Psychiatry. 2011;35(6):1461–71.
79. Marissal-Arvy N, Gaumont A, Langlois A, Dabertrand F, Bouchecareilh M, Tridon C, Mormede P. Strain differences in hypothalamic–pituitary–adrenocortical axis function and adipogenic effects of corticosterone in rats. J Endocrinol. 2007;195(3):473–84.
80. Campbell JE, Peckett AJ, D'souza AM, Hawke TJ, Riddell MC. Adipogenic and lipolytic effects of chronic glucocorticoid exposure. Am J Physiol Cell Physiol. 2011;300(1):C198–209.
81. Lee MJ, Pramyothin P, Karastergiou K, Fried SK. Deconstructing the roles of glucocorticoids in adipose tissue biology and the development of central obesity. Biochim Biophy Acta Mol Basis Dis. 2014;1842(3):473–81.
82. Lee RS, Tamashiro KL, Yang X, Purcell RH, Harvey A, Willour VL, Huo Y, Rongione M, Wand GS, Potash JB. Chronic corticosterone exposure increases expression and decreases deoxyribonucleic acid methylation of Fkbp5 in mice. Endocrinology. 2010;151(9):4332–43.
83. Neis VB, Bettio LB, Moretti M, Rosa PB, Olescowicz G, Fraga DB, Gonçalves FM, Freitas AE, Heinrich IA, Lopes MW, Leal RB, Rodrigues ALS. Single administration of agmatine reverses the depressive-like behavior induced by corticosterone in mice: comparison with ketamine and fluoxetine. Pharmacol Biochem Behav. 2018;173:44–50.
84. Jeon SW, Kim YK. Neuroinflammation and cytokine abnormality in major depression: cause or consequence in that illness? World J Psychiatry. 2016;6(3):283.
85. Moda-Sava RN, Murdock MH, Parekh PK, Fetcho RN, Huang BS, Huynh TN, Witztum J, Shaver DC, Rosenthal DL, Alway EJ, Lopez K, Meng Y, Nellissen L, Grosenick L, Milner TA, Deisseroth K, Bito H, Kasai H, Liston C. Sustained rescue of prefrontal circuit dysfunction by antidepressant-induced spine formation. Science. 2019;364(6436): eaat8078.
86. Orrico-Sanchez A, Chausset-Boissarie L, Alves de Sousa R, Coutens B, Rezai Amin S, Vialou V, Louis F, Hessani A, Dansette PM, Zornoza T, Gruszczynski C, Giros B, Guiard BP, Acher F, Pietrancosta N, Gautron S. Antidepressant efficacy of a selective organic cation transporter blocker in a mouse model of depression. Mol Psychiatry. 2020;25(6):1245–59.
87. Yu T, Li Y, Hu Q, Wang F, Yuan S, Li C, Li J, Cui J, Shen H. Ketamine contributes to the alteration of Ca^{2+} transient evoked by behavioral tests in the prelimbic area of mPFC: a study on chronic CORT-induced depressive mice. Neurosci Lett. 2020;735: 135220.
88. Brown LH, Strauman T, Barrantes-Vidal N, Silvia PJ, Kwapil TR. An experience-sampling study of depressive symptoms and their social context. J Nerv Ment Dis. 2011;199(6):403–9.
89. Elmer T, Stadtfeld C. Depressive symptoms are associated with social isolation in face-to-face interaction networks. Sci Rep. 2020;10(1):1444.
90. Nezlek JB, Imbrie M, Shean GD. Depression and everyday social interaction. J Pers Soc Psychol. 1994;67(6):1101.
91. Nezlek JB, Hampton CP, Shean GD. Clinical depression and day-to-day social interaction in a community sample. J Abnorm Psychol. 2000;109(1):11.
92. Baddeley JL, Pennebaker JW, Beevers CG. Everyday social behavior during a major depressive episode. Soc Psychol Pers Sci. 2013;4(4):445–52.
93. Vasconcelos AS, Oliveira ICM, Vidal LTM, Rodrigues GC, Gutierrez SJC, Barbosa-Filho JM, Vasconcelos SMM, de França Fonteles MM, Gaspar DM, de Sousa FCF. Subchronic administration of riparin III induces antidepressive-like effects and increases BDNF levels in the mouse hippocampus. Fund Clin Pharmacol. 2015;29(4):394–403.
94. Capibaribe VCC, Vasconcelos Mallmann AS, Lopes IS, Oliveira ICM, de Oliveira NF, de Castro Chaves R, Fernandes ML, de Araujo MA, da Silva DMA, Valentim JT, Maia Chaves Filho AJ, Macêdo DM, de Vasconcelos SMM, de Carvalho AMR, de Sousa FCF. Thymol reverses depression-like behaviour and upregulates hippocampal BDNF levels in chronic corticosterone-induced depression model in female mice. J Pharm Pharmacol. 2019;71(12):1774–83.
95. de Castro CR, Mallmann ASV, de Oliveira NF, Capibaribe VCC, da Silva DMA, Lopes IS, Valentim JT, Barbosa GR, de Carvalho AMR, de França

Fonteles MM, Gutierrez SJC, Filho JMB, de Sousa FCF. The neuroprotective effect of Riparin IV on oxidative stress and neuroinflammation related to chronic stress-induced cognitive impairment. Horm Behav. 2020;122: 104758.
96. Yu XD, Zhang D, Xiao CL, Zhou Y, Li X, Wang L, He Z, Reilly J, Xiao ZY, Shu X. P-Coumaric acid reverses depression-like behavior and memory deficit via inhibiting AGE-RAGE-mediated neuroinflammation. Cells. 2022;11(10):1594.
97. Darcet F, Mendez-David I, Tritschler L, Gardier AM, Guilloux JP, David DJ. Learning and memory impairments in a neuroendocrine mouse model of anxiety/depression. Front Behav Neurosci. 2014;8:136.
98. Patel SS, Udayabanu M. Urtica dioica extract attenuates depressive like behavior and associative memory dysfunction in dexamethasone induced diabetic mice. Metab Brain Dis. 2014;29(1):121–30.
99. Moreno LCGEAI, Solas M, Martínez-Ohárriz MC, Muñoz E, Santos-Magalhães NS, Ramirez MJ, Irache JM. Pegylated nanoparticles for the oral delivery of nimodipine: pharmacokinetics and effect on the anxiety and cognition in mice. Int J Pharm. 2018;543(1–2):245–56.
100. Kv A, Madhana RM, Bais AK, Singh VB, Malik A, Sinha S, Lahkar M, Kumar P, Samudrala PK. Cognitive improvement by vorinostat through modulation of endoplasmic reticulum stress in a corticosterone-induced chronic stress model in mice. ACS Chem Neurosci. 2020;11(17):2649–57.
101. Zborowski VA, Sari MH, Heck SO, Stangherlin EC, Neto JS, Nogueira CW, Zeni G. p-Chloro-diphenyl diselenide reverses memory impairment-related to stress caused by corticosterone and modulates hippocampal [3H] glutamate uptake in mice. Physiol Behav. 2016;164:25–33.
102. Lim DW, Park J, Jung J, Kim SH, Um MY, Yoon M, Kim YT, Han D, Lee C, Lee J. Dicaffeoylquinic acids alleviate memory loss via reduction of oxidative stress in stress-hormone-induced depressive mice. Pharmacol Res. 2020;161: 105252.
103. Mallmann ASV, de Castro Chaves R, de Oliveira NF, Oliveira ICM, Capibaribe VCC, Valentim JT, da Silva DMA, Sartori DP, Rodrigues GC, Maia Chaves Filho AJ, Riello GB, de França Fonteles MM, Vasconcelos SMM, Macedo D, Gutierrez SJC, Barbosa Filho JM, de Carvalho AMR, de Sousa FCF. Is Riparin III a promising drug in the treatment for depression? Eur J Pharm Sci. 2021;162: 105824.
104. Lim DW, Han D, Lee C. Pedicularis resupinata extract prevents depressive-like behavior in repeated corticosterone-induced depression in mice: a preliminary study. Molecules. 2022;27(11):3434.
105. Oliveira ICM, Mallmann ASV, de Paula Rodrigues FA, Vidal LMT, Sales ISL, Rodrigues GC, de Oliveira NF, de Castro CR, Capibaribe VCC, de Carvalho AMR, de França Fonteles MM, Gutierrez SJC, Barbosa-Filho JM, de Sousa FCF. Neuroprotective and antioxidant effects of Riparin I in a model of depression induced by corticosterone in female mice. Neuropsychobiology. 2022;81(1):28–38.
106. Inagaki R, Moriguchi S, Fukunaga K. Aberrant amygdala-dependent fear memory in corticosterone-treated mice. Neuroscience. 2018;388:448–59.
107. Deacon RM, Rawlins JNP. T-maze alternation in the rodent. Nat Protoc. 2006;1(1):7–12.
108. Gawel K, Gibula E, Marszalek-Grabska M, Filarowska J, Kotlinska JH. Assessment of spatial learning and memory in the Barnes maze task in rodents—methodological consideration. Naunyn-Schmiedeberg's Arch Pharmacol. 2019;392:1–18.
109. Cheung SG, Goldenthal AR, Uhlemann AC, Mann JJ, Miller JM, Sublette ME. Systematic review of gut microbiota and major depression. Front Psychiatry. 2019;10:34.
110. Barandouzi ZA, Starkweather AR, Henderson WA, Gyamfi A, Cong XS. Altered composition of gut microbiota in depression: a systematic review. Front Psychiatry. 2020;11:541.
111. Morais LH, Schreiber HL, Mazmanian SK. The gut microbiota–brain axis in behaviour and brain disorders. Nat Rev Microbiol. 2021;19(4):241–55.
112. Tanca A, Manghina V, Fraumene C, Palomba A, Abbondio M, Deligios M, Silverman M, Uzzau S. Metaproteogenomics reveals taxonomic and functional changes between cecal and fecal microbiota in mouse. Front Microbiol. 2017;8:391.
113. Ericsson AC, Gagliardi J, Bouhan D, Spollen WG, Givan SA, Franklin CL. The influence of caging, bedding, and diet on the composition of the microbiota in different regions of the mouse gut. Sci Rep. 2018;8(1):1–13.
114. Aizawa E, Tsuji H, Asahara T, Takahashi T, Teraishi T, Yoshida S, Ota M, Koga N, Hattori K, Kunugi H. Possible association of *Bifidobacterium* and *Lactobacillus* in the gut microbiota of patients with major depressive disorder. J Affect Disord. 2016;202:254–7.
115. Chen JJ, Zheng P, Liu YY, Zhong XG, Wang HY, Guo YJ, Xie P. Sex differences in gut microbiota in patients with major depressive disorder. Neuropsychiatr Dis Treat. 2018;14:647.
116. Marin IA, Goertz JE, Ren T, Rich SS, Onengut-Gumuscu S, Farber E, Wu M, Overall CC, Kipnis J, Gaultier A. Microbiota alteration is associated with the development of stress-induced despair behavior. Sci Rep. 2017;7(1):43859.
117. Wong ML, Inserra A, Lewis MD, Mastronardi CA, Leong LEX, Choo J, Kentish S, Xie P, Morrison M, Wesselingh SL, Rogers GB, Licinio J. Inflammasome signaling affects anxiety-and depressive-like behavior and gut microbiome composition. Mol Psychiatry. 2016;21(6):797–805.
118. Huang R, Wang K, Hu J. Effect of probiotics on depression: a systematic review and meta-analysis of randomized controlled trials. Nutrients. 2016;8(8):483.
119. Tian P, O'Riordan KJ, Lee YK, Wang G, Zhao J, Zhang H, Cryan JF, Chen W. Towards a psychobiotic therapy for depression: *Bifidobacterium breve* CCFM1025 reverses chronic stress-induced depressive symptoms and gut microbial abnormalities in mice. Neurobiol Stress. 2020;12: 100216.
120. Moya-Pérez A, Perez-Villalba A, Benítez-Páez A, Campillo I, Sanz Y. *Bifidobacterium* CECT 7765 modulates early stress-induced immune, neuroendocrine and behavioral alterations in mice. Brain Behav Immun. 2017;65:43–56.
121. Agusti A, Moya-Perez A, Campillo I, Montserrat-De La Paz S, Cerrudo V, Perez-Villalba A, Sanz Y. *Bifidobacterium pseudocatenulatum* CECT 7765 ameliorates neuroendocrine alterations associated with an exaggerated stress response and anhedonia in obese mice. Mol Neurobiol. 2018;55:5337–52.
122. Kelly JR, Borre Y, O'Brien C, Patterson E, El Aidy S, Deane J, Kennedy PJ, Beers S, Scott K, Moloney G, Hoban AE, Scott L, Fitzgerald P, Ross P, Stanton C, Clarke G, Cryan JF, Dinan TG. Transferring the blues: depression-associated gut microbiota induces neurobehavioural changes in the rat. J Psychiatr Res. 2016;82:109–18.
123. Liu Y, Zhang L, Wang X, Wang Z, Zhang J, Jiang R, Wang X, Wang K, Liu Z, Xia Z, Xu Z, Nie Y, Lv X, Wu X, Zhu H, Duan L. Similar fecal microbiota signatures in patients with diarrhea-predominant irritable bowel syndrome and patients with depression. Clin Gastroenterol Hepatol. 2016;14(11):1602–11.
124. Zheng P, Zeng B, Zhou C, Liu M, Fang Z, Xu X, Zeng L, Chen J, Fan S, Du X, Zhang X, Yang D, Yang Y, Meng H, Li W, Melgiri ND, Licinio J, Wei H, Xie P. Gut microbiome remodeling induces depressive-like behaviors through a pathway mediated by the host's metabolism. Mol Psychiatry. 2016;21(6):786–96.
125. Liu P, Gao M, Liu Z, Zhang Y, Tu H, Lei L, Wu P, Zhang A, Yang C, Li G, Sun N, Zhang K. Gut microbiome composition linked to inflammatory factors and cognitive functions in first-episode, drug-naive major depressive disorder patients. Front Neurosci. 2022;15: 800764.
126. Yu M, Jia H, Zhou C, Yang Y, Zhao Y, Yang M, Zou Z. Variations in gut microbiota and fecal metabolic phenotype associated with depression by 16S rRNA gene sequencing and LC/MS-based metabolomics. J Pharm Biomed Anal. 2017;138:231–9.
127. Zhang K, Fujita Y, Chang L, Qu Y, Pu Y, Wang S, Shirayama Y, Hashimoto K. Abnormal composition of gut microbiota is associated with resilience versus susceptibility to inescapable electric stress. Transl Psychiatry. 2019;9(1):231.
128. Wang X, Eguchi A, Fujita Y, Wan X, Chang L, Yang Y, Shan J, Qu Y, Ma L, Shirayama Y, Mori C, Yang J, Hashimoto K. Abnormal compositions of gut microbiota and metabolites are associated with susceptibility versus resilience in rats to inescapable electric stress. J Affect Disord. 2023;331:369–79.
129. Jiang H, Ling Z, Zhang Y, Mao H, Ma Z, Yin Y, Wang W, Tang W, Tan Z, Shi J, Li L, Ruan B. Altered fecal microbiota composition in patients with major depressive disorder. Brain Behave Immun. 2015;48:186–94.
130. Zheng S, Zhu Y, Wu W, Zhang Q, Wang Y, Wang Z, Yang F. A correlation study of intestinal microflora and first-episode depression in Chinese patients and healthy volunteers. Brain Behav. 2021;11(8): e02036.
131. Zhao H, Cheng N, Zhou W, Chen S, Wang Q, Gao H, Xue X, Wu L, Cao W. Honey polyphenols ameliorate DSS-induced ulcerative

colitis via modulating gut microbiota in rats. Mol Nutr Food Res. 2019;63(23):1900638.
132. Wen X, Wang HG, Zhang MN, Zhang MH, Wang H, Yang XZ. Fecal microbiota transplantation ameliorates experimental colitis via gut microbiota and T-cell modulation. World J Gastroenterol. 2021;27(21):2834.
133. Dong L, Du H, Zhang M, Xu H, Pu X, Chen Q, Luo R, Hu Y, Wang Y, Tu H, Zhang J, Gao F. Anti-inflammatory effect of Rhein on ulcerative colitis via inhibiting PI3K/Akt/mTOR signaling pathway and regulating gut microbiota. Phytother Res. 2022;36(5):2081–94.
134. Hamilton MK, Boudry G, Lemay DG, Raybould HE. Changes in intestinal barrier function and gut microbiota in high-fat diet-fed rats are dynamic and region dependent. Am J Physiol Gastrointest Liver Physiol. 2015;308(10):G840–51.
135. Liu W, Crott JW, Lyu L, Pfalzer AC, Li J, Choi SW, Yang Y, Mason JB, Liu Z. Diet-and genetically-induced obesity produces alterations in the microbiome, inflammation and Wnt pathway in the intestine of Apc+/1638N mice: comparisons and contrasts. J Cancer. 2016;7(13):1780.
136. Velázquez KT, Enos RT, Bader JE, Sougiannis AT, Carson MS, Chatzistamou I, Carson JA, Nagarkatti PS, Nagarkatti M, Murphy EA. Prolonged high-fat-diet feeding promotes non-alcoholic fatty liver disease and alters gut microbiota in mice. World J Hepatol. 2019;11(8):619.
137. Yang Y, Zhang Y, Xu Y, Luo T, Ge Y, Jiang Y, Shi Y, Sun J, Le G. Dietary methionine restriction improves the gut microbiota and reduces intestinal permeability and inflammation in high-fat-fed mice. Food Funct. 2019;10(9):5952–68.
138. Howren MB, Lamkin DM, Suls J. Associations of depression with C-reactive protein, IL-1, and IL-6: a meta-analysis. Psychosom Med. 2009;71(2):171–86.
139. Kohler O, Krogh J, Mors O, Benros ME. Inflammation in depression and the potential for anti-inflammatory treatment. Cur Neuropharmacol. 2016;14(7):732–42.
140. Pariante CM. Why are depressed patients inflamed? A reflection on 20 years of research on depression, glucocorticoid resistance and inflammation. Eur Neuropsychopharmacol. 2017;27(6):554–9.
141. Köhler-Forsberg O, Lydholm CN, Hjorthøj C, Nordentoft M, Mors O, Benros ME. Efficacy of anti-inflammatory treatment on major depressive disorder or depressive symptoms: meta-analysis of clinical trials. Acta Psychiatr Scand. 2019;139(5):404–19.
142. Alves A, Bassot A, Bulteau AL, Pirola L, Morio B. Glycine metabolism and its alterations in obesity and metabolic diseases. Nutrients. 2019;11(6):1356.
143. Altamura C, Maes M, Dai J, Meltzer HY. Plasma concentrations of excitatory amino acids, serine, glycine, taurine and histidine in major depression. Eur Neuropsychopharmacol. 1995;5:71–5.
144. Mitani H, Shirayama Y, Yamada T, Maeda K, Ashby CR Jr, Kawahara R. Correlation between plasma levels of glutamate, alanine and serine with severity of depression. Prog Neuropsychopharmacol Biol Psychiatry. 2006;30(6):1155–8.
145. Ogawa S, Koga N, Hattori K, Matsuo J, Ota M, Hori H, Sasayama D, Teraishi T, Ishida I, Yoshida F, Yoshida S, Noda T, Higuchi T, Kunugi H. Plasma amino acid profile in major depressive disorder: analyses in two independent case-control sample sets. J Psychiatr Res. 2018;96:23–32.
146. Ho CSH, Tay GWN, Wee HN, Ching J. The utility of amino acid metabolites in the diagnosis of major depressive disorder and correlations with depression severity. Int J Mol Sci. 2023;24(3):2231.
147. Dai ZL, Wu G, Zhu WY. Amino acid metabolism in intestinal bacteria: links between gut ecology and host health. Front Biosci. 2011;16(5):1768–86.
148. Wang W, Wu Z, Dai Z, Yang Y, Wang J, Wu G. Glycine metabolism in animals and humans: implications for nutrition and health. Amino Acids. 2013;45:463–77.
149. Martin FPJ, Wang Y, Sprenger N, Holmes E, Lindon JC, Kochhar S, Nicholson JK. Effects of probiotic *Lactobacillus paracasei* treatment on the host gut tissue metabolic profiles probed via magic-angle-spinning NMR spectroscopy. J Proteome Res. 2007;6(4):1471–81.
150. Luscher B, Shen Q, Sahir N. The GABAergic deficit hypothesis of major depressive disorder. Mol Psychiatry. 2011;16(4):383–406.
151. Fogaça MV, Duman RS. Cortical GABAergic dysfunction in stress and depression: new insights for therapeutic interventions. Front Cell Neurosci. 2019. https://doi.org/10.3389/fncel.2019.00087.
152. Robbins TW, Roberts AC. Differential regulation of fronto-executive function by the monoamines and acetylcholine. Cereb Cortex. 2007;17(suppl_1):i151–60.
153. Klinkenberg I, Sambeth A, Blokland A. Acetylcholine and attention. Behav Brain Res. 2011;221(2):430–42.
154. Craig SA. Betaine in human nutrition. Am J Clin Nutr. 2004;80(3):539–49.
155. Ueland PM. Choline and betaine in health and disease. J Inherit Metab Dis. 2011;34:3–15.
156. Hamlin JC, Pauly M, Melnyk S, Pavliv O, Starrett W, Crook TA, James SJ. Dietary intake and plasma levels of choline and betaine in children with autism spectrum disorders. Autism Res Treat. 2013;2013:1–7.
157. Ohnishi T, Balan S, Toyoshima M, Maekawa M, Ohba H, Watanabe A, Iwayama Y, Fujita Y, Tan Y, Hisano Y, Shimamoto-Mitsuyama C, Nozaki Y, Esaki K, Nagaoka A, Matsumoto J, Hino M, Mataga N, Hayashi-Takagi A, Hashimoto K, Kunii Y, Kakita A, Yabe H, Yoshikawa T. Investigation of betaine as a novel psychotherapeutic for schizophrenia. EBioMedicine. 2019;45:432–46.
158. Mischoulon D, Fava M. Role of *S*-adenosyl-L-methionine in the treatment of depression: a review of the evidence. Am J Clin Nutr. 2002;76(5):1158S-S1161.
159. Di Pierro F, Orsi R, Settembre R. Role of betaine in improving the antidepressant effect of *S*-adenosyl-methionine in patients with mild-to-moderate depression. J Multidiscip Healthc. 2015;8:39.
160. Kim SJ, Lee L, Kim JH, Lee TH, Shim I. Antidepressant-like effects of lycii radicis cortex and betaine in the forced swimming test in rats. Biomol Ther. 2013;21(1):79.
161. Lin JC, Lee MY, Chan MH, Chen YC, Chen HH. Betaine enhances antidepressant-like, but blocks psychotomimetic effects of ketamine in mice. Psychopharmacology. 2016;233(17):3223–35.
162. Mirzaei R, Bouzari B, Hosseini-Fard SR, Mazaheri M, Ahmadyousefi Y, Abdi M, Jalalifar S, Karimitabar Z, Teimoori A, Keyvani H, Zamani F, Yousefimashouf R, Karampoor S. Role of microbiota-derived short-chain fatty acids in nervous system disorders. Biomed Pharmacother. 2021;139: 111661.
163. Zierer J, Jackson MA, Kastenmüller G, Mangino M, Long T, Telenti A, Mohney RP, Small KS, Bell JT, Steves CJ, Valdes AM, Spector TD, Menni C. The fecal metabolome as a functional readout of the gut microbiome. Nat Genet. 2018;50(6):790–5.
164. Nolen-Hoeksema S. Sex differences in unipolar depression: evidence and theory. Psychol Bull. 1987;101(2):259–82.
165. Weissman MM, Bland RC, Canino GJ, Faravelli C, Greenwald S, Hwu HG, Joyce PR, Karam EG, Lee CK, Lellouch J, Lépine JP, Newman SC, Rubio-Stipec M, Wells JE, Wickramaratne PJ, Wittchen H, Yeh EK. Cross-national epidemiology of major depression and bipolar disorder. JAMA. 1996;276(4):293–9.

Publisher's Note